DEVELOPMENT OF A SECONDARY AIR CALCULATION TOOL FOR BUBBLING FLUIDIZED BED BOILER DESIGN

Lappeenranta–Lahti University of Technology LUT

Master’s Programme in Energy Technology, Master's thesis

2022

Aaro Nironen

Examiners: Adjunct Professor, D. Sc. (Tech) Kari Myöhänen
Associate Professor, D. Sc. (Tech) Jouni Ritvanen

Supervisors: M.Sc. (Tech) Pasi Liimatainen
M.Sc. (Tech) Toni Suutarinen

ABSTRACT

Lappeenranta–Lahti University of Technology LUT

LUT School of Energy Systems

Your degree programme: Energy Technology

Aaro Nironen

Development of a secondary air calculation tool for bubbling fluidized bed boiler design

Master's thesis

2022

73 pages, 24 figures, and 8 tables

Examiners: Adjunct Professor D. Sc. (Tech) Kari Myöhänen

Associate Professor D. Sc. (Tech) Jouni Ritvanen

Keywords: Bubbling fluidized bed boiler, secondary air system, jet penetration length, fluidized bed

Ever-increasing pressure to make environmentally conscious decisions has caused increased interest in biomass and waste combustion, resulting in risen demand of bubbling fluidized bed boilers. Sumitomo SHI FW is a global provider of energy systems and solutions, specializing in fluidized bed combustion units. The risen demand has in turn led to SHI FW wanting to update their BFB-related tools and guidelines.

Emission requirements and fuel choice are important factors affecting the air system design. A well-designed combustion air system helps to reach strict emission limits without the need for secondary emission removal systems. It also allows having good combustion conditions and performance even with more difficult fuels.

The main goal of this thesis was to develop an Excel-based calculation tool to dimension secondary air nozzles for BFB projects of SHI FW. The tool was simultaneously required to be simple to use while including features to support more advanced design choices. The theory of BFB boilers specializing in air systems was studied in support of the development process. One of the goals was to study the theory of nozzle jet penetration lengths to find out an improved way to evaluate them during the secondary air calculation process.

An effort was made to test 6 available penetration length correlations found in scientific literature. The inability to accurately determine suspension densities proved problematic during the study. Two of the correlations proved to be worthy of interest but validating them for use requires further evaluation. In the final calculation tool, an updated version of the old evaluation method was used. The finished calculation tool was tested, and it was successfully used during ongoing boiler proposal calculations.

TIIVISTELMÄ

Lappeenrannan–Lahden teknillinen yliopisto LUT

LUT Energiajärjestelmät

Energiatekniikka

Aaro Nironen

Sekundääri-ilman laskentatyökalun kehittäminen kuplapetikattilan suunnitteluun

Enegiatekniikan Diplomityö

2022

73 sivua, 24 kuvaa ja 8 taulukkoa

Tarkastajat: Adjunct Professor, D. Sc. (Tech) Kari Myöhänen

Associate Professor, D. Sc. (Tech) Jouni Ritvanen

Avainsanat: Kuplapetikattila, sekundääri-ilma, suihkun tunkeutuvuus, leijupeti

Kasvava paine tehdä ympäristöystävällisia ratkaisuja on lisännyt kiinnostusta biomassan ja jätteiden hyötykäyttöön energiantuotannossa, mikä on johtanut kasvaneeseen kuplapetikattiloiden kysyntään. Sumitomo SHI FW on kansainvälinen energiajärjestelmien ja ratkaisujen valmistaja, joka on erityisesti tunnettu leijupetikattiloistaan. Kysynnän kasvu on vuorostaan johtanut SHI FW:n päivittämään kuplapetikattiloiden suunnitteluun liittyviä työkalujaan.

Ilmajärjestelmän suunnitteluun vaikuttavat erityisesti käytetty polttoaine ja päästötavoitteet. Hyvin suunniteltu palamisilmajärjestelmä auttaa pääsemään päästötavotteisiin ilman kalliita lisäjärjestelmiä. Se on myös edellytys hyvän palamisen aikaansaamiseksi hankalia polttoaineita käyttäessä, ja se säästää kattilan käyttöönottoon ja säätöön kuluvaa työpanosta.

Tämän työn päätarkoitus oli kehittää Excel pohjainen kuplapetikattilan sekundääri-ilmasuutinten mitoitus- ja laskentatyökalu SHI FW:n käyttöön. Työkalulta toivottiin yksinkertaisuutta ja helppokäyttöisyyttä, mutta sen tuli myös olla kykenevä ottamaan huomioon monimutkaisempia suunnitteluvalintoja. Kuplapetikattiloiden yleistä teoriaa tutkitkittiin kehitysprosessin tueksi, ilmajärjestelmiin painottuen. Tavoitteena oli myös löytää parempi tapa sekundääri-ilmasuihkujen tunkeutuvuuden arviointiin.

Työssä testattiin kuutta tieteellisessä kirjallisuudessa saatavilla ollutta suihkun tunkeutuvuuden laskukaavaa. Ongelmia aiheuttivat vaikeudet suspensiotiheyden määrittelyssä. Tutkimuksen perusteella korrelaatioista kaksi oli kiinnostavia, mutta niiden käyttö laskentatyökalussa vaatisi lisätutkimusta. Itse laskentatyökalussa päädyttiin käyttämään aiemmin käytetyn tunkeutuvuuslaskennan paranneltua versiota. Valmis työkalu on testattu toimivaksi ja sitä käytettiin onnistuneesti uuden kattilan tarjousprosessin aikana.

SYMBOLS AND ABBREVIATIONS

Roman characters

d_j	jet diameter	[m]
d_p	particle diameter	[m]
h	elevation	[m]
k	loss coefficient	[-]
L	jet penetration length	[m]
m	mass	[kg]
p	pressure	[bar, Pa]
q_v	volume flow	[m^3/s]
q_m	mass flow	[kg/s]
R_s	specific gas constant	[J/molK]
T	temperature	[ºC, K]
U	velocity	[m/s]
U_c	suspension velocity	[m/s]
U_j	jet velocity	[m/s]
V	volume	[m^3]
v	velocity	[m/s]

Greek characters

α	decay constant	[m^{-1}]
ε	volume fraction	[-]
ρ_c	suspension density	[kg/m^3]

ρ_{fb}	freeboard gas density	[kg/m^3]
ρ_j	gas jet density	[kg/m^3]
ρ_p	particle density	[kg/m^3]

Constants

g	gravitational acceleration	9.81 m/s

Subscripts

abs	absolute
air	air
nozzles	nozzles
NTP	conditions at 0 ℃ and 101 325 Pa
mix	mixture of air and recirculated flue gas
pipe	pipe

Abbreviations

ADP	Acid Dew Point
BFB	Bubbling Fluidized Bed
CFB	Circulating Fluidized Bed
CFD	Computational Fluid Dynamics
ESP	Electrostatic Precipitator
FB	Fluidized Bed
FG	Flue Gas
FGR	Flue Gas Recirculation

HVAC	Heating Ventilation and Air Conditioning
ID	Induced Draft
LHV	Lower Heating Value
MSW	Municipal Solid Waste
PA	Primary Air
PC	Pulverized Combustion
RCG	Re-Circulation Gas
RDF	Refuse Derived Fuel
SA	Secondary Air
SCAH	Steam Coil Air Heater
SCR	Selective Catalytic Reduction
SNCR	Selective Non-Catalytic Reduction
SRF	Solid Recovered Fuel
TA	Tertiary Air
VBA	Visual Basic for Applications

Table of contents

1 Introduction

1.1 Background

The development of fluidized bed gasification started in the early 1920s by Fritz Winkler. However, it took until the 1960s before the first fluidized bed combustion (FBC) test units emerged. They have since proven to be a favourable technology to combust solid fuels, such as coal and biomass. The main idea of FBC is to replace a traditional combustion grate with a bed of fine solids, which is then fluidized by blowing air through a grid of nozzles located at the bottom of the furnace. The Bubbling fluidized bed boiler (BFB) was developed first, with the earliest industrial units appearing in the 1970s. However, it was proven to be unfavourable for coal combustion, which was, and currently is, a prevalent fuel for large-scale power generation. Circulating fluidized bed boilers with increased fluidizing air velocity were commercialized shortly after, in the 1980s, and have since then been competing with pulverized coal combustion, which still is the most popular boiler type for large scale power generation. (Koornneef et al., 2007)

Despite being a less advanced technology compared to CFBs, BFB boilers have held their share of the steam boiler market, mainly due to the rising interest in using carbon-neutral biomass as a fuel for energy and heat generation. Typical biofuels, such as forest industry residues, require short transport distances to be economically viable, which has driven the need for boiler solutions in smaller size classes. BFB boilers are mechanically simpler while possessing many of the advantages of fluidized beds, such as low emissions, good combustion efficiency, and fuel flexibility. These advantages compared to their lower capital costs make them desirable especially for small sized biomass- and waste combustion plants.

BFB boilers contain most of the typical components in all modern steam boilers, including a furnace, convective heat transfer surfaces, a water circulation system, and auxiliary systems, including emission control- and ash handling systems. Its air system is more complex in comparison to more traditional boiler types, due to the need for fluidization air. Secondary air acts as combustion air fed above the bed in the upper regions of the furnace, having a significant impact on combustion conditions, enabling better combustion efficiency and less emissions. The ability to reach desired emission requirements without

installing costly secondary removal systems allows cutting capital costs. A well-designed air system allows stable operation, thus promoting better availability of the boiler.

1.2 Research objectives

This master's thesis work has been conducted in partnership with the Sumitomo SHI FW's offices in Varkaus. SHI FW is a global provider of energy generation solutions and has a long history especially in providing and developing fluidized bed systems. The main goal of this thesis is to develop an Excel-based calculation tool, used for secondary air nozzle dimensioning by Sumitomo SHI FW during the performance calculations of its BFB boiler projects. The tool is required to give precise results while being user-friendly and intuitive to use. A Major emphasis in the work is placed on studying the theory of nozzle jet penetration. Available methods found in scientific literature are tested to determine if they can be utilized to calculate penetration lengths in BFB boiler freeboard.

The theoretical part of this thesis aims to provide a basis of knowledge of most concepts and components related to the BFB boilers, with emphasis on the air system and the factors which highlight the importance of successful secondary air design. Theoretical considerations which are used as the basis of the air system dimensioning are studied based on available scientific literature and studies in addition to SHI FW's own materials. Air systems can also often be overlooked or briefly discussed in typical steam boiler textbooks. In addition to the calculation tool development, this work attempts to provide more detailed information on the most important concepts regarding BFB air systems, especially directed towards students and other individuals interested in the field of energy technology.

1.3 Research methods and structure

The research of this work is based on the review of scientific literature, and internal materials of SHI FW. Some previous CFD simulation results are utilized as a part of the work, but none are created due to the limitations of the schedule. This work can be roughly divided into 4 sections:

1. Introduction
2. Theory
3. Study of methods for measuring jet penetration length
4. Presentation of results.

The introduction aims to give a brief background of the work discussing fluidized bed combustion and the importance of combustion air systems. After this, the theory of BFB boilers is discussed in chapters 2 and 3. The air system and its most important components are introduced in chapter 4, while chapter 5 contains a discussion of theoretical considerations behind the air system design. The concept of jet penetration length is closely adjacent to the secondary air design, and studies of the literature on the subject can be found in chapters 5 and 6. This study includes calculations with six available jet penetration length correlations. A presentation and discussion of the results can be found in chapter 6. Finally, chapter 7 contains a description of the final calculation tool that was developed.

2 Fluidized bed combustion

Fluidized bed boilers have become an increasingly popular choice for industrial and commercial heat and power generation. When a new modern power- or heating plant utilizing biofuels is considered, the used boiler type is often chosen between a grate or either bubbling- or circulating fluidized bed. Due to their versatility in offering solutions for a wide range of fuels and large size range, fluidized bed boilers have been able to become a dominant option over grate firing, except for specific niche fuels, which have too high alkali content to properly combust in a fluidized bed (Pena, 2011). Circulating fluidized beds are also a prevalent option for large-scale coal combustion units, competing with the more traditional and popular pulverized coal combustion (PC) technology.

2.1 Fundamentals of fluidization

Fluidized beds used in energy generation processes are based on injecting air to the bottom of a bed of fine solid material, to make it attain a fluid-like state. This means that the bed's behaviour is comparable to the behaviour of a liquid, for example, the fluidized material can be drained almost like water from a vessel and the bed surface stays horizontal even if the bed is tilted. The main benefits of fluidization regarding the combustion are temperature uniformity and increased heat transfer capabilities. The bed material can retain a lot of heat, which allows the inserted fuel to dry fast and burn at a fixed temperature. Most of the benefits seen in fluidized bed combustion units compared to traditional boilers are related to the use of the bed and its gas-solid interactions, which highlights the importance of a proper understanding of the bed operation. (Basu, 2006, p. 21; Scala, 2013)

To obtain this fluid-like state for the bed material, the gravitational forces acting on the bed particles must be counteracted with drag forces generated by the fluidizing air. Characteristics of the bed are mainly influenced by the bed material properties and the velocity of the fluidizing air. Based on the air velocity, different bed states can be divided to five regimes: packed bed (a), bubbling bed (b,) turbulent bed (c), fast/circulating bed (d) and, transport bed (e). The aforementioned fluidization regimes can be seen demonstrated in figure 1. (Basu, 2006, p. 21)

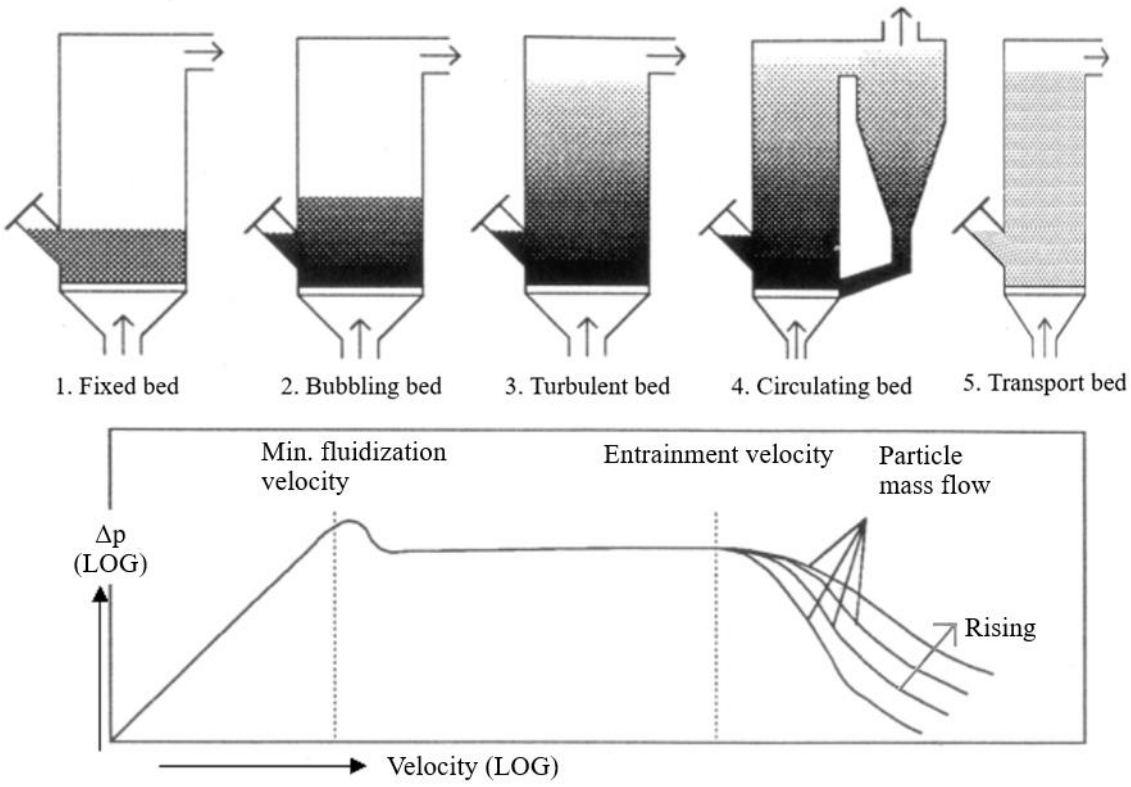

Figure 1. Fluidization regimes from lowest air velocity to the highest and corresponding figure of pressure loss related to fluidizing velocity. (Adapted from Raiko et al., 1995.)

While the fluidization air velocity stays low enough, the bed remains in packed state. Particles of a packed bed remain stationary while the gas flows through them. To move the bed from packed to bubbling state, the fluidization velocity must reach the minimum bubbling velocity, which is a bit higher than the minimum fluidization velocity. The bubbling state is characterized by the bubbles that form in the bed from the excess gas and rise through the bed "emulsion". A bubbling bed has a clear, visually identifiable surface. (Basu, 2006, pp. 26–28)

The rise of fluidization velocity expands the bed, eventually leading to a change in the fluidization regime. A turbulent bed is characterized by with an increased fraction of bubbles that rapidly form and break, diffused but still identifiable bed surface, and the rise of the rate of entrained bed material. If the fluidization velocity is raised even further, fast fluidization regime (referred to as circulating bed in figure 1) is achieved. This results in particles and particle clusters becoming continuously entrained with the fluidization air stream. The minimum velocity requirement for a fast bed is known as transport velocity. (Basu, 2006, pp. 27–38)

2.2 Fluidized bed boilers

Fluidized bed boilers can be divided into two main types: circulating fluidized bed (CFB) boilers and bubbling fluidized bed (BFB) boilers. BFB boilers have an established bed level around the elevation of 1 m due to their lower fluidizing air velocity, which limits the particles from being able to become entrained with the flue gas flow and allows the bed to remain in a bubbling state. CFB boilers have higher fluidization velocity and smaller bed particle sizes. This allows them to operate in the fast or circulating fluidized bed region characterized by high particle entrainment rate out of the bed. Due to this, a way to separate solids from the flue gas stream is required to maintain operation. In the figure below, there can be seen a cyclone used as a hot solid separator in CFB and an additional heat transfer surface used to extract heat from circulated material (both highlighted with a circle). The required furnace size for equal power output is also smaller for CFB compared to BFB. (Vakkilainen, 2016, p. 212)

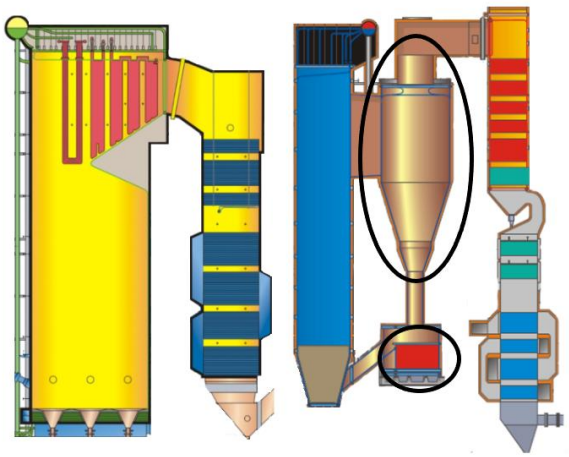

Figure 2. Furnace and flue gas path schematic of BFB (SFW) compared to CFB (Valmet). (Adapted from SHI FW internal materials, 2022.)

Vakkilainen (2016) mentions 0.7-2.0 m/s as the optimal range of fluidization velocity and 0.5-1.5 mm as the optimal range for bed particle diameter for BFB boilers. Respective values for CFB boilers are 3-10 m/s and 0.1-0.5 mm. Sand is often used as the initial bed material used for fluidized bed systems. However, ash resulting from the combustion process and possible sorbent (limestone) insertion will add up and change the composition of the bed. In a CFB which has been in constant operation, the fraction of sand can be very

low, as the solids recirculation and limestone feeding replenish the bed inventory without makeup sand. In BFBs there is no similar recirculation system, and the role of make-up sand is higher in maintaining the bed inventory. However, there can also be a system in place to recirculate fine bottom ash back to bed. (Basu, 2006, p. 6-10, p. 212)

Advantages typically associated with both FBB types are fuel flexibility, high combustion efficiency, and low emissions compared with good additional removal options for both sulphur and nitrogen oxides to meet the highest emission standards. Basu (2006, p. 6) mentioned values up to 96 % and 99.5 % for the combustion efficiencies of BFB and CFB respectively. However, modern units are capable of higher efficiencies, especially when firing biomass. Based on the bed material's inherent ability to store heat, FBBs are not susceptible to sudden changes in fuel quality. This was well demonstrated by Basu (2006, p. 10) by comparing PC and CFB firing of coal: a sudden 10 % fluctuation in ash content of the fuel will cause serious disturbance and problems to the operation of a PC unit while a CFB unit can handle this type of changes without problems.

In addition, there are some BFB- and CFB-specific features to consider. For example, CFB is easier to scale into large utility plants, partly due to its smaller furnace cross-section area. BFB requires around 2-3 times more grid area to produce the same heat output. In turn, BFBs don't require a solid separator and are cheaper and easier to manufacture (Basu, 2015, pp. 8–15). It must also be remembered that the efficient combustion zone of BFB for solid fuel particles is mostly limited to the lower furnace. In a CFB most of the furnace allows good combustion conditions due to the circulation mechanism, which lowers the losses resulting from fine unburned fuel particles. During fluidized bed operation the bed particles come frequently in contact with boiler surfaces, providing more efficient heat transfer. This effect is more prevalent in CFBs, as in BFB boilers the furnace is covered with refractory at the elevations where there is a meaningful amount of bed particles present. In BFB boilers, most of the heat transfer is based on flame radiation through uncovered tubes in the freeboard. (Scala, 2013) (Basu, 2006, p. 11)

CFB has proven to be more favorable than BFB, especially in large utility boilers which still often operate with fossil fuels. It can reach the best efficiency values and the strictest emission standards while offering the best capabilities for flexible multi-fuel firing. An inherent recirculation system and longer combustion zone help in burning char left in fly ash, which is especially advantageous when firing coal, which is still common around the

world in large scale power generation units. BFB boilers perform worse efficiency-wise and they tend to run into problems with rising bed temperatures during coal combustion, which has made them mostly obsolete for that purpose. (Scala, 2013, p. 642)

Based on the last few paragraphs, it's easy to draw a conclusion that CFB is the superior technology of the two FB options. This raises the question "What drives the demand for BFB boilers?". The simplest reasoning is that most of the downsides associated with BFBs compared to CFB are not present when considering the use of biomass fuels. Due to the higher share of volatiles in biomass, there is less char to be burned in the bed, which does limit the excessive rise of bed temperatures. This helps to abandon the impractical in-bed heat transfer tubes and promotes better availability (Basu, 2006, p. 216). The higher combustion efficiency of CFBs has more importance the more expensive fuel is fired. Biomass fuels are inherently cheaper than high-grade coal for example, which makes the worse combustion efficiency of BFBs less significant.

There is always evident interest in lowering the capital costs of any power and heat generation systems. BFB boilers can perform reasonably close compared to CFB regarding emissions and efficiency, while the construction is simpler and cheaper. While being comparable in terms of required capital costs, grate boilers have higher maintenance cost mostly due to the moving parts of the grate. These factors make BFB technology a very competitive and often favorable choice when considering a boiler for biomass combustion, especially in cases under the size of 100 MW_{el}. (Pena, 2011)

2.3 Solid fuel combustion

Aside from oil/gas burners required for boiler start-up and load support, BFB boilers operate using solid fuels. Combustion of solid fuels can be simplified to occur in four identifiable stages: drying, volatile release (devolatilization), volatile combustion, and char combustion. Incombustible parts of the fuel referred to as ash, are left behind. These stages will often overlap considerably, especially for large biomass particles (Raiko et al., 1995, p. 139). Base values for the time scales of each combustion stage, for a biomass particle with diameter of 2 mm, can be found in table 1.

Table 1. Time scales of combustion of a 2 mm biomass particle. (Vakkilainen, 2016, p. 35)

Combustion stage	Time scale (s)
Drying	0.05-0.2
Devolatilization	0.1-0.3
Char combustion	0.2-10
Ash reactions	Long

When a fuel particle is inserted into the furnace it starts to heat immediately. Shortly after the water content of the particle will start evaporating. Drying occurs fast in FB boilers due to the heat retained in the bed material, even if the fuel was high moisture biomass. The bed and overall furnace temperatures are over 800 °C (apart from part-load scenarios) which is a lot higher than the water vaporization temperature. This makes heat transfer the main limiting factor for drying and volatilization. (Raiko et al., 1995, pp. 143–147)

During devolatilization, light gases (can be referred to as "volatile matter") such as CO, H_2, CH_4, CH6, and C_6H_6 release from the heated fuel particles. The share of the volatile compounds is high in both biomass and peat, around 80 % and 70-80 % for wood and peat respectively, which are fuels typically burned in BFBs. For coal, this share is from 10-40 % depending on its grade. Combustion of volatiles occurs partly in the bed, but mainly in the freeboard above, which is where secondary combustion air is fed. The share of volatiles of the fuel used is very essential to consider, as a high share of them increases the importance of secondary air in combustion control. On the other hand, the use of fuels with a low share of volatiles shifts the load of the combustion process more towards bed area. (Vakkilainen, 2016, pp. 32–35), (Raiko et al., 1995, pp. 143–147)

In addition to combustible matter, part of the nitrogen and sulphur content of the fuel releases during devolatilization. Nitrogen forms compounds such as HCN and NH_3 which then react with oxygen forming NO. This mechanism is only partly dependent on the combustion temperature, while the amount of oxygen present has a large impact on the forming of emissions. If HCN and NH_3 form in sub-stoichiometric conditions, they mostly form N_2 instead. Due to this, the division of combustion air (air staging) is an effective method for the reduction of the emissions from the volatile nitrogen. The most important emission forming sulphur compound in the sub-stoichiometric conditions is H_2S, which is reduced mainly by using sorbents, such as limestone. (Raiko et al., 1995, pp. 247-251)

After the devolatilization and combustion of volatiles, the fuel particle is mostly reduced to char and ashes. Most of the char composition is carbon, but it also contains up to 0.5 %

oxygen and hydrogen, 0.5-1 % nitrogen, and up to half of the total sulphur in coal. The last two elements are known to form notable emission compounds such as NO and SO_2. Combustion of the char takes place in the bed, and it's a slower process compared to the combustion of volatiles. During this process, oxygen available in the bed reacts with the carbon of the char either on the surface of the particle or inside its pores. (Perry et al., 1997, p. 27-5)

Ash content refers to the share of incombustible material which is either an inherent part of the fuel or is foreign material that is acquired during the harvesting and processing of the fuel. An example of the latter is dirt incorporated to wood fuels, which can account for a high share of its total ash content. Even though incapable of combustion, many compounds in ash will continue to react further in high furnace temperatures. Ash reactions are important to consider, as some can be very harmful, causing sintering and agglomeration in the bed or corrosion and fouling of heat transfer surfaces. (Azad and Rasul, 2019), (Khan, 2009)

3 Bubbling fluidized bed boiler

Apart from small hot-water boilers used for district heating, the main purpose of a typical BFB boiler is to produce superheated steam, which can be then used to generate power and/or heat. Energy for this is acquired through combusting solid fuels in the furnace, where water is first turned to a mixture of saturated water and steam in the furnace wall tubing. The mixture flows to a separator referred to as the drum, from where steam moves onwards to superheaters and water continues back to the furnace wall tubes.

Flue gases resulting from the combustion process flow through the convective heat transfer section on their way to flue gas treatment, before being released to the atmosphere through a stack. Hot flue gases are used to superheat the steam in superheaters, to preheat the water in the economizer, and finally to preheat combustion air in the air preheater. Combustion air is divided into primary air used to fluidize the bed and secondary air used as additional combustion air fed in furnace above the bed.

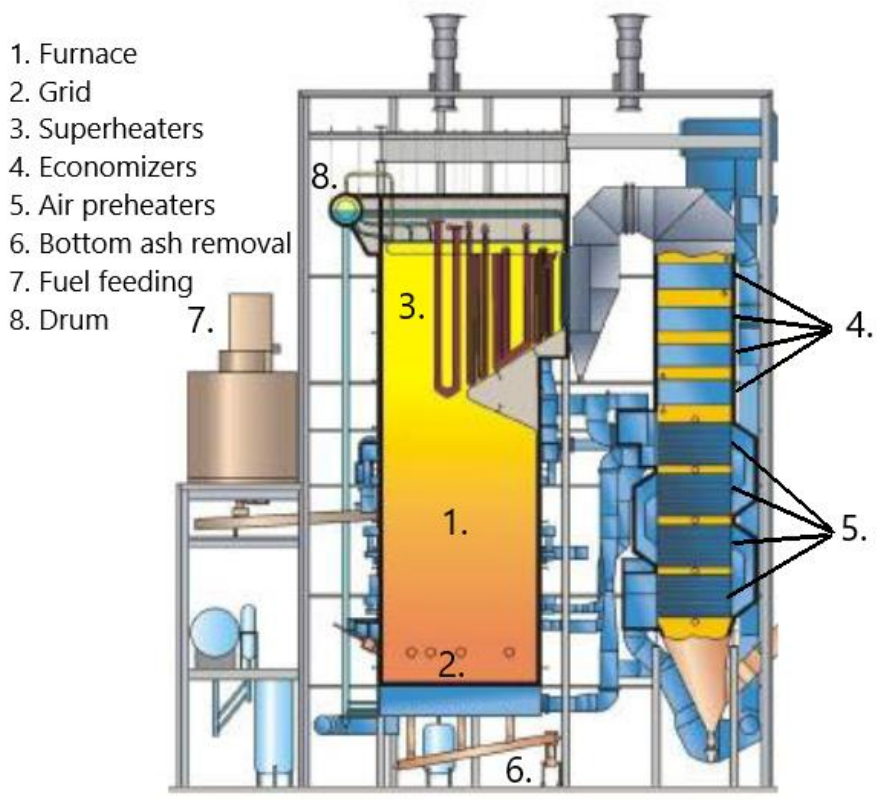

Figure 3. Sample BFB boiler (Adapted from SHI FW internal materials, 2020).

A cross-section view of a typical BFB boiler with most of the important components numbered can be seen in figure 3. They contain similar systems compared to any traditional boiler. A typical convective heat transfer section with superheaters, economizer, and air preheating package can be seen, along with other important components such as the drum, based on which water/steam circulation is built around.

3.1 Water/steam circulation

Most, if not all, modern BFB boilers are made with natural or forced water and steam circulation. They differ from each other in the method by which water is transported to the evaporator. In natural circulation systems transport is driven by the density difference between the cold water in the downcomer pipes and the water and steam mixture in the upcomer pipes in the furnace wall. This allows the heated mixture to flow back to the drum. In forced circulation, the same process is assisted by a pump which is located at least a few meters under the drum to avoid cavitation. Typically, it is located towards the bottom end of downcomers. A simplified description of both drum-based circulation methods and once-through circulation, which is introduced later, can be seen in figure 4. (Huhtinen, 2000, pp. 113–118)

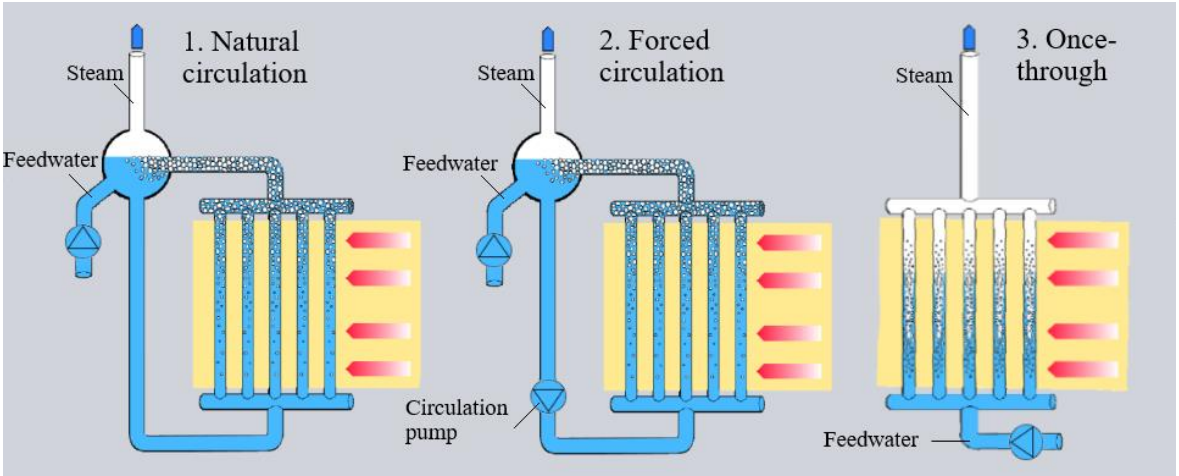

Figure 4. Natural- forced-, and once-through water/steam circulation. **(**Adapted from SHI FW internal materials, 2022.)

The main components for both drum-based circulation methods include a feedwater tank, pump, drum, feedwater preheater (economizer), evaporator (furnace), and superheaters. Water is transported from the feedwater tank and is heated close to its saturation

temperature in the economizer. Almost saturated feedwater is led by downcomers from drum to risers where part of it evaporates before it heads back. The drum acts as a separator between feedwater and saturated steam. Steam rises to the top of the drum and naturally transports to superheaters, where it is superheated to its end temperature and water continues back to the wall tubing. (Huhtinen, 2000, pp. 113–118)

Using a drum-based circulation method limits the available main steam pressure to subcritical pressures, as supercritical water does not have clearly defined phases that can be separated in the drum. The so-called once-through method can be utilized in boilers where it is beneficial for steam pressures to reach the supercritical range (>209.9 bar). In a once-through boiler seen in figure 4, feedwater flows to evaporator pipes straight from the economizer and continues then to superheaters. It is most often used in large-scale coal power plants, where the considerable increase of total efficiency (from around 34 % to 40+ %) from higher steam temperatures can offer noticeable economic and environmental advantages. These supercritical units are CFB or PC boilers rather than BFB, where drum-based circulation is practically the only method used. (Huhtinen, 2000, p. 120)

3.2 Heat transfer surfaces

Furnace is the area in which the combustion occurs and it’s responsible for transferring heat to feedwater, turning it into saturated steam. Furnace walls are made from a water tube membrane which is protected by a thick layer of refractory in the lower part of the furnace, as it’s the area most prone to erosion due to the proximity to the bed material. Refractory also stores heat, which partly helps with regulating bed temperature. Bed temperatures are often limited between 700 – 850 °C. The bottom temperature limit is based on being able to fully burn all the fuel, while the upper limit is determined by the need to avoid agglomeration of bed material. In the freeboard temperatures rise higher, while often being limited to around 1000 °C. (Vakkilainen 2016 s. 217-220)

Traditionally, there has been an option to build in-bed heat exchanger tubing inside the furnace of a BFB boiler. This is included in older designs for coal combustion, to lower bed temperature to an acceptable range (under 850 °C) while simultaneously extracting the heat to the steam. Expectedly, placing heat transfer surfaces under constant impingement of hot bed material makes them extremely vulnerable to corrosion and erosion. Using lower fluidization velocity and vertical finned tubes can reduce these detriments. Overall,

using bed tubes in a BFB boiler is questionable at best and it is avoided altogether in modern biomass combustion units. This is done by avoiding high bed temperatures by using sub-stoichiometric air amounts in the bed area, which is not possible when coal is the main fuel. (Basu, 2006, pp. 240–249)

The area after the bed to the upper regions of the furnace is often referred to as “freeboard”. The main load of furnace heat transfer in the tube membrane walls occurs in the freeboard through flame radiation. In addition to this, the combustion of volatiles takes place mostly in the freeboard, which accounts for a major fraction of the combustion process, especially when burning biomass or other fuels that contain a lot of volatile matter. Secondary combustion air nozzles and possible ammonia injection nozzles are also located at freeboard elevations.

After the freeboard ends, the flue gases flow to an area often referred to as the backpass or the convective section. This area contains all convective heat transfer surfaces, of which superheaters are located closest to the furnace. They are used to superheat the saturated steam generated in the furnace tubing, which increases the process efficiency and dries the steam. Superheaters can be categorized as “convective” or “radiative”. Most of the superheaters in BFBs are convective type and are protected from flame radiation, either being in the backpass or after the furnace “neck”. Radiation superheaters are located to the furnace closer to, or even in midst of the combustive zones, which requires them to be able withstand harsher conditions and higher temperatures. An example configuration could be one radiation superheater coupled with two convective units. (Teir, 2003, p. 10)

Economizers are located after superheaters, which are used to heat feedwater to its saturation temperature utilizing thermal energy left in flue gases after superheaters. The low temperature of the flue gases allows economizer construction to have leniency in spacing, and to consider the use fins to maximize heat transfer properties. However, biomass combustion is associated with the tendency of fouling the heat transfer surfaces. They are a usual fuel choice for BFB boilers and in such cases, a looser tube spacing and unfinned tubes are recommended. (Teir, 2003, p. 8; Vakkilainen, 2016, p. 131 & p. 171)

After economizers, there is often an air preheating package. They are naturally the most important heat transfer surfaces regarding air systems. Besides increasing the total efficiency of the boiler process, preheating of combustion air increases the stability of the

furnace operation. Air preheaters are often the last surface in the flue gas path used, to utilize the last obtainable thermal energy left in the flue gas stream. Most designs also include a steam coil air preheater (SCAH), using low-pressure steam (4-10 bar) to heat the combustion air before the actual air preheater. SCAH is typically used when achieving the desired air temperature would result in flue gases cooling to too low temperatures after the FG air preheater. (Huhtinen, 2000, p. 201; Vakkilainen, 2016, p. 172)

The temperature limit of flue gas cooling depends mostly on the acid dew point (ADP), which is in turn dependent on the sulphur content of the fuel used, but it is generally around 130-150 ℃. If the temperatures under the ADP are reached, the acidic compounds in the flue gas condense to heat transfer surfaces, causing harmful low-temperature corrosion. The most likely surfaces to be affected are the air preheater and flue gas ducts, but it can even occur in the economizer. (Huhtinen, 2000, p. 100 and p. 201)

Flue gas air preheaters are typically divided into either recuperative or regenerative types based on their operating principle. In the recuperative FG-preheater, heat is transferred from the flue gases to air directly through the heat exchanger surfaces. They are typically tubular, but a plated design is also possible. Recuperative air heaters require a large surface area as the heat transfer coefficients between two gases are naturally very low. They also require sootblowing for cleaning. Regenerative preheaters employ an additional heat-storing material that stores heat from the hot flue gases and transfers it to the air. They require less space in comparison but are more prone to leakage between the hot and cold sides. Recuperative preheaters are cheaper and more convenient for small boilers, such as BFB boilers. In large-scale CFB and PC power generation units the cost of materials required to provide enough heat transfer surface can become so high, that the regenerative preheaters can become the economically more attractive option. (Vakkilainen, 2016, pp. 171–173).

3.3 Auxiliary systems

3.3.1 Emissions and corresponding control methods

Along with CO_2, the most typical emissions that require consideration during boiler operation are CO, NO_x, SO_x, and particulate emissions. CO_2 is the most famous greenhouse gas it's emitted from all combustion processes. CO is nontoxic gas however known for its

ability to prevent proper oxygen circulation in the human respiratory system. CO is produced through incomplete combustion of fuel, in other words, when there is not enough oxygen present. It's not necessarily harmful in the sense of air pollution but is most importantly monitored for the sake of the combustion process and to control other emissions. High amounts of CO in flue gases indicate that the process does not operate correctly, and combustion air is insufficiently present or poorly mixed. (Vakkilainen, 2016, p. 50)

After all possible heat is extracted from the hot flue gases, it needs to be released into the atmosphere. Before this can be done, harmful particle emissions need to be reduced below the allowed emission limits. The main systems used for particle removal are fabric filters and electrostatic precipitators (ESP). ESP is based on creating electric current on wires which negatively charge passing particles. This makes them gravitate towards plates, which are in turn charged positively. Fabric filters often called bag filters, use permeable material which collects ash particles on its surface. Deposits formed on the surface further help in filtering particles out of the flue gases. (Vakkilainen, 2016, pp. 160–162)

The most important nitrogen-related emissions consist of NO (nitric oxide) and N_2O (nitrous oxide). NO has a short life in the atmosphere (under an hour), where it reacts with oxygen, forming NO_2. Due to this, both NO_2 and NO are often referred to collectively as NO_x. NO_2 is toxic to humans, and it accelerates ozone (O_3) formation in lower regions of the atmosphere. Ozone acts as a greenhouse gas, is harmful to humans, and is one of the main components of the smog found in urban areas. N_2O is also a significant greenhouse gas. (Vallero, 2014, pp. 520–524), (Vakkilainen, 2016, p. 49)

NO_x emissions are divided into two distinct categories based on which they are formed: thermal NO_x and fuel NO_x. Thermal variety is a result of reactions between nitrogen and oxygen during high-temperature operation in furnaces. Fuel NO_x consists of oxides produced during the combustion process from the nitrogen content of the fuel (Vallero, 2014, p. 888). Thermal NO_x generation is essentially zero in modern BFB boilers due to their low operating temperatures and the main focus in reduction is aimed at the fuel NO_x. (Vakkilainen, 2016, p. 49).

In an ideal scenario, most of the nitrogen oxide emission control in BFBs is done using so-called primary techniques, which are based on directly impacting the combustion process.

Typical methods for this are air staging, flue gas recirculation, and combustion with low-excess air, which highlights the role of air system design. If required emission limits for NO_x can't be met using primary techniques, secondary techniques are introduced. Selective non-catalytic reduction (SNCR) and selective catalytic reduction (SCR) are the two main options. They are based on the injection of ammonia or urea into the upper furnace or flue gas ducts, which then reacts with the nitrogen forming mostly harmless compounds. SCR systems also include a reactor unit on the flue gas path, which contains a catalyst to accelerate the reduction process. (Vallero, 2014, pp. 888–891)

Sulphur is abundantly present in our earth's lithosphere and thus often found in fuels, especially in coal but also to a lesser extent in biomass. It reacts with oxygen during combustion, and the resulting gases (SO_2 and SO_3) cause pollution which results in the acidification of soil. Dry or wet scrubbing is a traditional method to reduce these emissions. During wet scrubbing, flue gases flow through a wet scrubber which employs a mixture of limestone and water to react with the sulphur oxides providing harmless calcium sulfate. Wet scrubbers can reach SO_2 removal rates of over 90 %. (Vakkilainen, 2016, p. 45), (Vallero, 2014, p. 888)

However, especially in fluidized bed combustion, lime (CaO) or limestone ($CaCO_3$) can be fed to the furnace for convenient control of SO_2 emissions. This results in calcination-sulfidation reaction forming harmless end products, such as $CaSO_4$. Sorbent insertion should be used as the main SO2 reduction method, as its cheaper and easier to implement. If it's not enough to reach the emission limits by itself, scrubbing should be considered. Overall, sulphur-related emissions aren't often problematic during the combustion of biomass fuels, simply due to their low sulphur content. (Scala, 2013, p. 658), (Vakkilainen, 2016, p. 45)

3.3.2 Fuel and ash handling

Solid biofuels often have low heating values and volumetric quantities required for plant operation are high. They require a large area to store and special considerations for the handling equipment. Biofuel feeding path includes typically the following systems:

- Fuel receival, storage, preprocessing area
- Smaller "day silos" with as low as 30-minute capacity during MCR operation

- Fuel conveyors to furnace
- Feeding chutes from the conveyors to furnace.

Fuel conveyers from the day silos operate with either drag-chain or screw conveyors, the latter of which can be found in smaller systems provided that the screw length from silo to furnace does not become excessively long. The fuel feeding chutes are equipped with mechanical rotary feeders supplying them with fuel from the conveyors. Feeding to the furnace consumes air from the air system to aid fuel movement, chute wall cooling, and launch fuel to the top of the bed.

In modern BFB boilers, fuel feeding is done above the bed from multiple feeding points. The number of openings is chosen case by case. The larger the bed area is, the more feeding points are required to allow even fuel distribution. Fuel insertion below the bed has also been studied as it increases the volatile combustion in the bed and could to control high freeboard temperatures. However, below bed insertion is not used, due to it causing unnecessary detriments. Use of it can result in worse fuel spreading, erosion problems, and excessive local bed cooling during the use of fuels with high moisture content. (Scala, 2013, p. 655)

Combustion residues from unburned fuels, referred to as ash, require considerations in the terms of their storage and disposal. In BFB operation ash is divided into the bottom- and fly ash. Fly ash is removed from the flue gas stream by methods mentioned in the last chapter (ESP & Bag filter) and bottom ash is continuously removed from the furnace bottom by cooled ash drains and screws. Particle size and composition are different between the two ash types, which affects the way how the ash can be recycled or where it is disposed of. They are often stored separately, especially in larger plants. (Vakkilainen, 2016, pp. 162–164)

3.3.3 Burners

Start-up burners are included in every BFB boiler design. They are typically used to slowly heat the bed material during the start-up process to provide a high enough temperature to start the combustion of solid fuels (400-600 °C). A slow start-up process is also designed to mitigate the temperature shock which would result from too fast temperature changes

and could lead to material damage. In addition to start-up burners, some designs also feature load burners. They are located upper in the furnace and are used to sustain sufficient furnace temperatures during part-load operation, during issues in the fuel feeding or when drastic increases in fuel moisture drive the bed temperature down. To some extent, start-up burners can also be used for the same purpose. (Vakkilainen, 2016, p. 164)

3.4 Typical fuel choices for BFB boilers

Typical fuels used in Sumitomo/Foster Wheeler provided BFB boilers and their characteristics can be seen in table 2. Other fuels for which BFBs are built to fire as a main fuel include sugar cane residue and eucalyptus. Different types of coal, RDF, agricultural wastes, and energy crops can also be used as a complementary fuel.

Table 2. Characteristics of typical fuels used in Sumitomo provided boilers. Fuels that can be traditionally fired alone can be seen in bold. (BFB references)

Fuel	Moisture [%]	Ash [%]	Sulphur [%]	LHV_{wet} [MJ/kg]
Wood Residue	45-55	1.4-2.2	0.02-0.05	7.1-9.2
Bark	58	2.3	0.07	7.8
Sawdust	55	1.5	0	7.2
Peat	45-53	4.7-7	0.11-0.2	8.5-10
RDF	15-30	7-8.5	0.2	15.8-16
De-Inking Sludge	37	42	0.18	7.0

Instead of large-scale coal burning power stations, BFB boilers are advantageous in smaller scale biomass and waste combustion units. Smaller plant sizes are driven by biomass and waste fuel sources being scarcely available while their transportation is not often economically viable over distances of 150-300 km. In small-scale operation, features of BFB boilers are desirable and their negative qualities are less relevant. For example, the inherent advantage of CFBs allowing the recirculation of unburned fuels is way less advantageous when burning biomass compared to coal. Most importantly, the lower capital costs combined with the lower efficiency of BFB units prove to be financially advantageous in smaller size classes when compared to CFB units, which have higher capital costs but better efficiency.

Waste and biomass fuels are both known as hard fuels to utilize be it their high moisture content, ash content, or quality variations. BFB boilers are known to be well suited for difficult fuels due to the flexibility of the operation. Biomass combustion also does not lead to too high bed temperatures in the same way as burning coal, essentially due to the

higher share of volatiles in biomass (80 % to 10-40 %), which shifts combustion out of the bed. The capability of retaining heat created by the bed material and refractory helps to mitigate and smoothen the temperature fluctuations, which fuel quality variations would otherwise create. BFB operation is also insensitive to differences in fuel particle sizes, only the fuel feeding system requires particle size quality to be in an acceptable range.

3.4.1 Biomass

Forest biomass is a typical example of biomass used in commercial heat and energy production units. Huhtinen (2002, pp. 72) mentions bark waste from wood peeling as the most used industrial biofuel (in Finland). The low energy density of wood makes it economically viable for only short transport distances, which makes energy production reliant on being locally tied to the proximity of the forest industry. Its use in energy generation is most prevalent in Nordic and Baltic countries, where forests are abundant. The ratio of forest area compared to total land is roughly 73.9 %, 66.9 % and, 53.9 % in Finland, Sweden, and Estonia respectively, which indicates local potential for forest biomass-based energy production. (Röser, 2008, pp. 10–12)

Forest residues consist of primary- and secondary residues. Primary residues are mostly excess wood from mass logging and other forestry operations. Secondary residues consist of forest industry wastes, for example, produced during the operation of pulp or board factories. This includes bark, sawdust, and wood shavings. Wood recycling also presents another fuel source especially from demolition and construction projects. All above-mentioned fuels have been featured either as a primary or at least a complimentary fuel in Sumitomo SHI FW provided BFB boilers. (Röser, 2008, p. 14)

Even though “biomass”, refers to a wide variety of different fuels, they share certain characteristics which make them difficult to utilize. They often have high moisture and volatile content and low heating value. In addition to this, there can be a large variance in fuel quality during the operation. Positive shared characteristics include low ash and sulphur content.

The chemical composition of the fuel determines which problematic detriments should be accounted for. Silicon (Si), potassium (K), aluminium (Al), iron (Fe), magnesium (Mg), and calcium (Ca) are among the most important ash-forming compounds in biomass. High

amounts of alkali (Si and K) lower the ash melting temperature, which leads to higher agglomeration tendency of bed material. The chlorine content of biomass fuels can often be high, which needs to be considered as it is a major cause of corrosion (Basu, 2006, p. 127). To properly account for these problems in the boiler design, careful analysis of the used fuel is required. (Khan, 2009)

3.4.2 Waste fuels

Along with different biomasses, waste fuels and sludges are possible to combust in BFB boilers. In Finland during the year 2018, almost 56 % of municipal solid waste was combusted in 9 dedicated waste combustion units and as a secondary fuel in 24 other units. Waste and sludge incineration can be considered primarily as a method to get rid of waste mass, while also providing energy. Processed waste fuels are often referred to as SRF (solid recovered fuel) or RDF (refuse-derived fuel) and are made from waste mass which has been filtered, dried, and shredded to a moderately uniform size. (Bröckl et al., 2021, pp. 15–20)

Table 3. SRF moisture and LHV variations between feedstocks. MSW is for Municipal Solid Waste, I&CW for Industrial and Consumer Waste, and C&DW for Construction and Demolition Waste. (Nasrullah et al., 2015.)

	MSW	SRF I	I&CW	SRF II	C&DW	SRF III
Ash (550 °C) [m-%]	22.4	9.8	16.6	12.5	46.8	9.0
Moisture [m-%]	13.5	15.0	26.5	25.0	12.0	16.5
LHV, wet [MJ/kg]	16.7	20.2	13.0	18.0	9.8	18.0

The quality of RDF always varies based on the type of waste used in its production, as can be seen in table 3. Alakangas et al. (2016) state the most important quality criteria as: “particle size, moisture, impurities, and chemical composition (chlorine, aluminum, and heavy metal content)”. The amount of heavy metals that can be found in particle emissions from waste combustion can be higher compared to clean biomass. Chlorine in RDF is a cause of high-temperature corrosion similar to wood fuels, while metal aluminum melts easily in furnace temperatures and then condenses on cooler heat transfer surfaces forming deposits. Careful fuel analysis and sufficient design to account for problems presented by the chosen fuel are required for successful operation. (Alakangas et al., 2016, pp. 148–164)

Sludge is a waste slurry, formed in several processes of the forest industry, agriculture, and water treatment. In Finland, municipal waste sludge is mostly used for soil improvement, and it has some potential for biogas production but is not very viable to directly combust for energy generation. However, around 60 % of forestry sludges were used for energy production (332 000 tons) in 2014. Sludges are characterized by their high moisture and varying ash content (up to 60-85 % and up to 60 %), which makes them hard to utilize as fuel. When used, they most typically account for only a small fraction of the total fuel mixture. To consider BFB operation with sludge as the main fuel, removal methods need to be employed to reach moisture levels of around 30-50 %. Even then, waste sludges are generally not viable as a sole primary fuel, at least for large-scale power generation. (Alakangas et al., 2016, pp. 165–168)

4 Air system description

Combustion air system has the utmost importance in all boiler operation, as the right amount of combustion air is necessary for good combustion efficiency and emission control. All modern BFB units employ some form of air staging, a method where combustion air is split between primary air (PA) and one or multiple secondary air (SA) stages. A typical share of PA from total combustion air is from 40 % to 60 %. In addition to combustion air, BFB-boilers require a system to supply fluidizing air for the bed operations, this makes the air system more complex compared to more traditional combustion methods, such as grate firing. (Scala, 2013, p. 654)

All components and systems required to supply fluidization and combustion air in BFB are included under the term “air systems”. In other words, this includes the whole path from air inlet ducts through fans and ducts to the furnace and auxiliary consumers. A typical pathway from air inlet duct to furnace consists of components such as a silencer, fan, ducting, measurements, and control dampers, while ending either in the windbox and grid in case of primary air, or the nozzles for secondary air. Air preheating package is also crucial part of all boiler operations and was addressed in the “heat transfer surfaces” -chapter (Vakkilainen, 2016, p. 60).

Several auxiliary systems require a constant supply of air to maintain their operation. This includes the start-up and load burners, fuel feeding systems and limestone-, fly ash- and bottom ash re-injection air. Some of the mentioned systems are more infrequently used, such as bottom ash re-injection, but start-up burners for example can be found in all BFB boilers.

4.1 Primary air

The most important purpose of the primary air system is to provide fluidizing of the bed through nozzles in the bottom grid, which simultaneously provides its share of the combustion air. The bed operation affects the operation as a whole and is responsible for most benefits BFB units have compared to other boiler types. This makes careful primary air design very important.

4.1.1 Fluidizing grid

Successful FB operation requires a system to supply the required amount of fluidization air to the bed at a sufficient velocity to reach the desired bed fluidization state. The simplest way to achieve this is to use a perforated or porous plate or simple-grate type construction with uniformly placed holes. They are simple, cheap, and easy to construct. However, this type of construction does not meet the requirements present in a modern, constantly operated commercial boiler. Perforated plates are used for simpler systems mostly in the field of academic research, due to the ease of setup process and low cost. (Basu, 2006, pp. 360–364)

In modern commercial units, the fluidizing grid is made from nozzles positioned uniformly in the furnace bottom. Preheated primary air is distributed to the nozzles through an air distribution system called the windbox. It is designed with the intent of providing equal distribution of the air with the minimum amount of pressure loss possible. The bottom nozzles must also be resistant to erosion, corrosion, and clogging due to the nature of the bed operation. Along with this, an option for constant removal of bottom ash and bed material needs to be included. Usually, this is done with plated or refractory lined ash drains placed based off the full bottom grid design. (Scala, 2013, pp. 654–660)

Traditional nozzle grid construction in FB boilers consists of nozzles of uniform height with a varying number of cooled ash drains located around the middle of the furnace bottom. The number and overall performance requirements of ash drains are chosen based on the fuel used and the dimensions of the furnace bottom. High alkali fuels require fluent and constant operation of the bottom ash removal. Simpler grid constructions can be considered, when the fuel contains low amounts of impurities and alkali, for example when firing peat or sugarcane residues.

To handle more problematic fuels with high amounts of coarse impurities, such as small metal objects or stones, a more advanced grid construction should be used. Most of the prominent BFB boiler manufacturers have their own grid designs, of which detailed information is confidential. For example, SHI FW has its Step Grid construction, based on arranging refractory protected horizontally blowing nozzles at equally stepped heights, allowing free flow of impurities towards ash drains. Valmet in turn has their Hydro Beam

construction, again designed for easy removal of bottom ash and impurities. (Valmet, 2022)

4.1.2 Flue gas recirculation

Flue gas recirculation (FGR) is a technology traditionally employed to minimize the formation of thermal NO_x. The method is based on lowering combustion temperatures by substituting oxygen-rich combustion air with nearly inert flue gases (recirculation gas, RCG), fed in low temperatures relative to the furnace. However, in BFBs the formation of thermal NO_x is practically zero due to low combustion temperatures, and FGR is instead used for bed temperature control. It's another system that is technically optional but is very often found in modern BFB boilers, as it's often the only feasible method for its purpose. In turn, maintaining sufficiently low bed temperature has the utmost importance in minimizing the agglomeration of bed material caused by melting ash. Excessive use of FGR should still be avoided as it lowers boiler efficiency and can raise furnace velocities needlessly. (Liimatainen, 2022, Vakkilainen, 2016, p. 153)

In BFBs, FGR is often mixed with the primary air stream to be fed from the fluidizing grid. The used flue gas is extracted after particle removal systems (ESP or bag filter) to provide it as clean as possible. However, there are always some particles present, thus a design that provides good self-cleaning capabilities should be chosen for the FGR fan. (Huhtinen, 2000, p. 243)

Some BFB designs, especially with certain waste fuels can require more attention to freeboard temperature control. While simply increasing the amount of the FGR to primary air will also lower furnace temperatures in the upper regions, excessive FGR feeding will result in unnecessarily cooling down the bed. A better option to lower temperature peaks in furnace upper regions is to implement FGR either to secondary air or from own designated nozzles. Use of it must be carefully considered, as the aforementioned downsides apply similarly to secondary FGR. It can also affect the fulfillment of the residence time requirements set for waste combustion (chapter 3.4). (Liimatainen, 2022)

4.2 Secondary air

Air staging is used to describe the division of combustion air to different levels. Most, if not all, modern BFB boilers employ some form of this. Additional combustion air beside the primary air is referred to as secondary air (SA). It is often further divided into two or three stages, depending on the furnace design. If a third secondary air stage is used, it is often called tertiary air (TA). This division allows the creation of sub-stoichiometric zones in the furnace, which is an effective method to control NO_x emissions (discussed also in chapter 2.3). It inhibits the combustion in the bed, thus limiting the bed temperatures as well. (Basu, 2006, p. 121)

Secondary air is fed to the furnace through nozzles located on the furnace wall. Typical SA nozzles are openings at a 90-degree angle, piercing the furnace membrane wall. One row of lower secondary air nozzles embedded in the boiler tube membrane wall can be seen in figure 5. The openings can be seen to be protected with refractory lining.

Figure 5. Lower secondary air nozzles of a new and clean BFB boiler (SHI FW internal material, 2022).

Secondary air design has an especially large impact on the performance of BFB boilers, which are mainly constructed to burn biomasses that contain a high share of volatiles in proportion to char. The bed is used to dry and devolatilize the fuel and while the char burns in the bed, most of the released volatiles complete their combustion in the freeboard above the bed. As it’s inserted in the freeboard of the furnace, secondary air design has a high impact in providing good conditions for efficient the combustion of volatiles. The locations

of SA stages also have an important role in emission control, especially in minimizing NO_x emissions. (Vakkilainen, 2016, p. 221) (Sher et al., 2017).

4.3 Air system equipment

To transport air properly to different consumers in the air system, a well-operating transport network is required. Fans draw their air from specific inlet ducts equipped with a silencer to minimize noise and then transport them forward in ducts towards the furnace and other air consumers. To ensure correct and constant air flows to every consumer, and overall stable operation of the air system, sufficient measurement and flow control systems must be in place.

4.3.1 Air ducts

Ducts are needed to transport air between different points of the power plant process. An example of the ducts from a SA fan to boiler walls can be seen in figure 6. Air ducts are required to be gas-tight and able to withstand under and over-pressures. Ducts are either circular or rectangular, barring transition points. The choice of cross-section geometry is based on both performance (cost, structural and fluid behaviour) and external limitations (space, equipment, and erection limitations). Circular ducts pose the following advantages compared to rectangular alternatives:

- Efficient in handling pressure loads (lower wall cost)
- Fewer stiffeners required (lower cost)
- Better fluid flow characteristics (lower pressure loss)
- Smaller perimeter (lower insulation costs).

They also pose the following disadvantages:

- Using equipment designed for rectangular ducts can require a lot of effort
- Even though their perimeter is lower, they need to be approximately 13 % wider (this can cause layout problems). (ASCE: Air and Gas Duct Structural Design Committee, 2020)

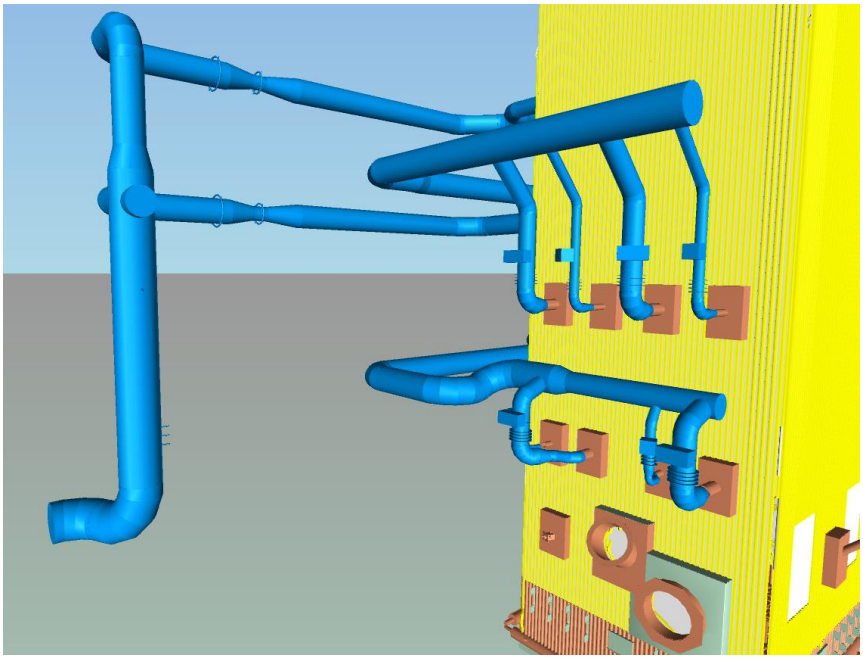

Figure 6. SA ducts (coloured in blue) from fan to one furnace wall (SHI FW Internal material, 2022).

Most air ducts used to provide primary- or secondary air in a modern boiler employ flow-altering devices (figure 7), such as turning vanes, splitters, baffles, or distribution plates. Their main function is to control the flow and to minimize unwanted effects such as turbulence or pressure drop. To combat thermal expansion, expansion joints are used. They are often placed close up or downstream to major systems and air consumers, such as fans, the boiler, and air heaters. All hot-side air ducts are also insulated, most commonly with fiberglass. (ASCE: Air and Gas Duct Structural Design Committee, 2020, p. 15)

Bends in the duct are a typical cause of pressure losses and uneven flow due to the disturbance they cause in the flow field. Turning vanes are used in duct bends to mitigate this effect by efficiently directing and dividing the flow. Besides bends and turns, the division of flow from a larger channel to smaller ones is another major cause of similar unwanted effects. To avoid this, splitter plates can be used to divide the flow more uniformly for the two resulting channels. (ASCE: Air and Gas Duct Structural Design Committee, 2020, pp. 183–185)

Distribution plates also known as perforated plates are often located in conjunction with large changes in duct cross-sectional area. They are made from plates pierced with patterned openings with an open area ratio of around 30-75 %. The plate applies resistance to the flow and helps in mitigating turbulent swirls and eddies. They help in providing a

uniform flow field across the duct when it's required, but a high amount of pressure loss is caused as a drawback. The local pressure losses from different parts of ductwork can add up quickly, which affects fan size requirements and raises internal consumption of electricity leading to higher costs. Due to this, the use of perforated plates needs to be carefully considered. (ASCE: Air and Gas Duct Structural Design Committee, 2020, p. 185).

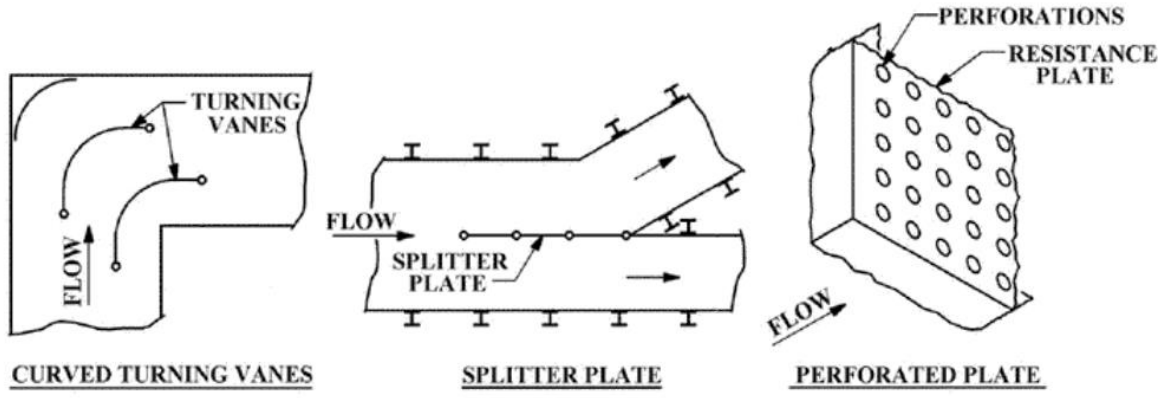

Figure 5. Simplified configurations of the most typical flow-altering devices. (Adapted from ASCE: Air and Gas Duct Structural Design Committee, 2020, p. 182)

Calculating pressure loss for all components on the expected air route, for example from the SA fan to the furnace inlet, is a very essential part of the air system design. This is done to obtain the required pressure difference for fan dimensioning. To obtain pressure losses in ducts caused by different elements specified above, typical pipe flow pressure loss equation can be used

$$\Delta p = (\frac{f_d L_{pipe}}{D} + \sum K) \frac{\rho v^2}{2} \quad (1)$$

where f_d is frictional pressure loss, L_{pipe} is length, D is hydraulic diameter, $\sum K$ is the sum of local losses, ρ is pressure loss and v is fluid velocity. Local losses are an umbrella term for all losses caused by local obstructions in the ducting, such as turns, valves, and dampers. Calculating local loss coefficients individually for each case is very rarely necessary and table values for different elements are abundantly available.

4.3.2 Fans

In BFB boilers the most essential fans are primary air fans, secondary air fans, flue gas fans, and flue gas recirculation fans. A typical characterisation of fan types is made between the flow angle after the impeller: axial and radial fans. Radial fans have an inlet along the shaft and feature an impeller with blades that turn the flow direction 90 degrees from axial to radial. Their axially operating counterpart moves the air parallel to the rotation. Radial fans are suited for higher pressures and are most often used in power plant applications. However, for applications that require lower pressures and are space-restricted, using axial fans could be considered case by case. (Huhtinen, 2000, pp. 245–247)

Fans used to extract flue gas out of the furnace are often so-called “induced draft”-type. The ID fans (or FG fans) used in BFB combustion units are typically located in the flue gas stream after flue gas treatment systems. Subsequently, by providing the draft for flue gases to exit, FG fans produce under-pressure in the furnace, which prevents the leakage of hot combustion gas inside the boiler building. (Vakkilainen, 2016, p. 119)

Typical blade shapes for radial fans include backward curved, forward curved, and straight blades (figure 8). Forward curved blades are specialized to provide a high flow rate combined with low pressure, which makes them only usable in HVAC applications (Heselton, 2014). Backward curved blades are best from an efficiency standpoint and are used whenever applicable. They are suited for clean gases, which makes them ideal to be used for both primary- and secondary air transport. However, when flue gas or air likely to contain dust is transported, radial type of blades should be considered. Radial outlet angle indicates good self-cleaning properties, which is necessary when dealing with gas with dust and fly ash. Careful aerodynamic design is especially important for flue gas fans and recirculation fans, as their unit sizes are large, and combining good efficiency and self-cleaning properties can be troublesome. (Huhtinen, 2000, p. 245)

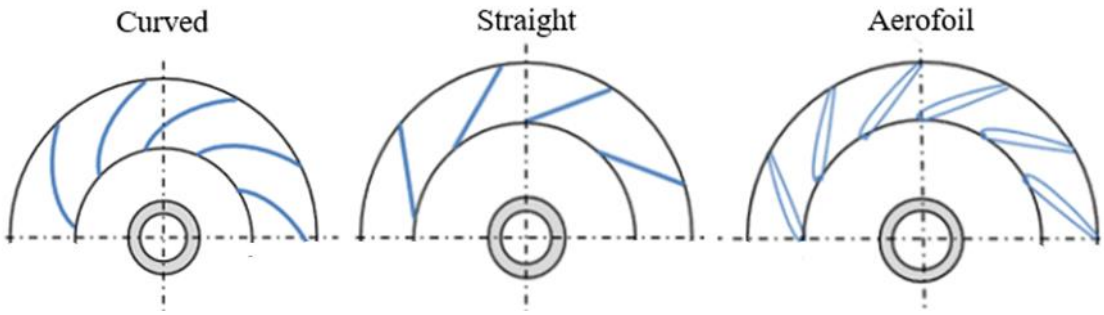

Figure 6. Backward curved impeller types. (Modified from SHI FW internal materials)

Typical control methods for fans are throttle or rotational speed control. Throttle control can be done by either limiting the air intake (inlet vane control) or installing a damper to the duct (damper control). Inlet vanes are a cheap and effective control method in the operational range of 50–100 %. The inlet vane method can go down even to 30 % but it then becomes increasingly bad for efficiency. Damper control is often only used only as an additional method paired with either speed or inlet vane control. Speed control can be implemented stepwise using a multi-speed motor or gearbox. Continuous speed control using a frequency converter is ideal regarding fan performance, but it has the highest capital costs. It is often used for PA fan control while normal speed control is sufficient for SA and FG fans. (Huhtinen, 2000, p. 245)

Required pressure difference and volume flow are calculated during the fan dimensioning to account for all pressure losses and air consumers on its air path. Fan efficiency and size are also to be considered. Fan manufacturers have their performance curves for each fan, which consist of total pressure change presented as a function of volume flow and rotational speed. During the fan selection, these curves are used to determine if a fan matches the requirements and operates suitably on typical loads in which the boiler is operated. Smaller fans can be often chosen from the catalogs of the manufacturers while larger SA and PA fans can be custom-made on demand. (Huhtinen, 2000, p. 245)

4.3.3 Flow measurements

Successful boiler operation requires a wide range of control and automation systems, which in turn operate using measurement data obtained from important process points. Flow measurements for combustion air system can be done at least with Venturi tube-,

aerofoil-, thermal mass flow- and averaging Pitot tube meter. Air flow measurements in BFB are found at least in the air ducts of most of the air consumers and before every fan. In an example scenario, this would include one for all stages of SA, fluidizing grid, FGR, and auxiliary consumers such as burners and fuel-feeding systems. (Lindsley et al., 2018, pp. 120–126)

The Venturi tube, Pitot tube, and aerofoil meters measure flow based on pressure differential. Their operation is based on so-called Bernoulli's principle which in simple terms states that static pressure should decrease during the rise of velocity to satisfy the conservation of energy. In Venturi tube flow is measured by constricting flow locally with pressure measurements set up before and after. This creates a pressure difference, from which the flow rate can be obtained. (Basu and Debnath, 2019, p. 241)

Most commonly air flow measurements in modern power plants are done using a Venturi tube. It sports a relatively high 1 % accuracy, and it is moderately cheap, tolerant to impurities, and has low to medium pressure loss. Venturi tube requires a uniform flow profile for accurate measurements, which in turn requires enough straight flow path before and after the measurement. Required distances vary around 5-20 and 5-10 times the tube cross-section, both upstream and downstream respectively. Cross section of a typical Venturi tube measurement can be seen in figure 9. (Basu and Debnath, 2019, pp. 242–245)

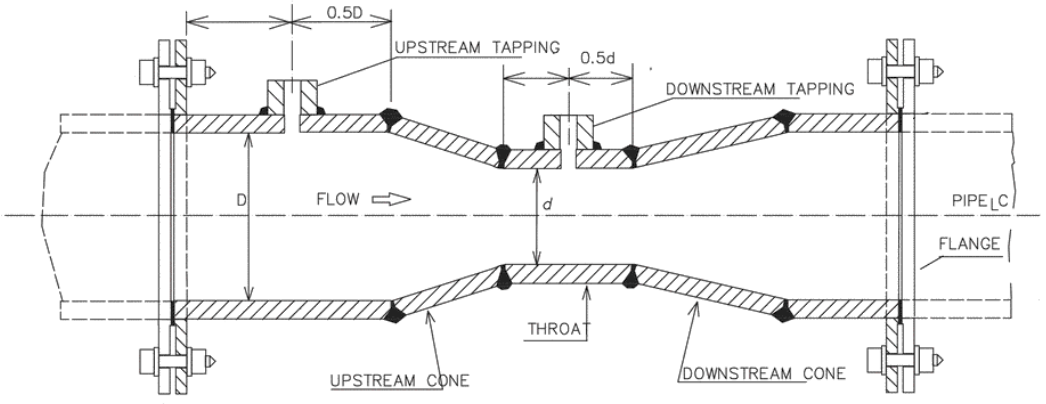

Figure 7. A Venturi tube cross-section. Tapping equals to pressure measurement. (Adapted from Basu and Debnath, 2019).

5 Considerations during secondary air system design

In this chapter, the theory behind the secondary air design is discussed based on both academic source material and SHI FW's internal materials. While the secondary air calculation tool developed in this work is mostly based around guidelines in the internal material, reviewing external sources is beneficial in the terms of achieving a more complete understanding of the subject.

The emission requirements and fuel choice are among the most important factors to consider during the air system design. Correct air staging helps in minimizing emissions and allows efficient combustion with difficult fuels. Improperly functioning combustion air system can lead to problems, especially during the plant commissioning, which can cause costly delays.

5.1 Air staging

Combustion air in BFB boilers is divided between primary and secondary air, with a primary air share of 40-60 % based on the design (Scala, 2013, p. 654). However, values around 40 % are more typical for modern units. The amount of primary air is essentially based on the fuel used. During the combustion of very wet fuels, increasing PA share can help to increase combustion in the bed and promote stable bed temperatures.

Secondary air is then split between 1-3 stages, which provide their share of combustion air according to the design. The vertical placement of the feeding zones varies between designs, but their function is generally similar. The lower SA feeding zone is located close to the fluidized bed to provide air for intensive combustion of the volatiles released from the fuel. Upper SA fed above this intensive zone to fully complete the combustion process. If a third SA level (tertiary air) is used, the load of the combustion process shifts upwards, and the TA takes up the role of fully completing the combustion. An example split between lower SA, upper SA, and TA stages could be 40/20/40. It must be noted that in other sources, the term TA can also be used to refer to the second SA level instead of the third.

The effect of combustion air can be demonstrated through the furnace temperature profile and combustion zones. A rough description of the combustion zones of a sample BFB furnace with two secondary air levels can be seen in figure 10. On the right it also includes

an estimation of a temperature profile of a biomass combusting BFB boiler. A constant temperature in bed elevation (around 0-1 m) can be observed, followed by a region of high temperature starting before and especially after the lower SA stage. This demonstrates well the accelerated combustion of volatiles after extra O_2 is inserted. Combustion completes after the last air feeding stage, after which there is still plenty of furnace height left for final reactions to complete. If SNCR/SCR is used, ammonia injection is typically located in the upper end of the freeboard.

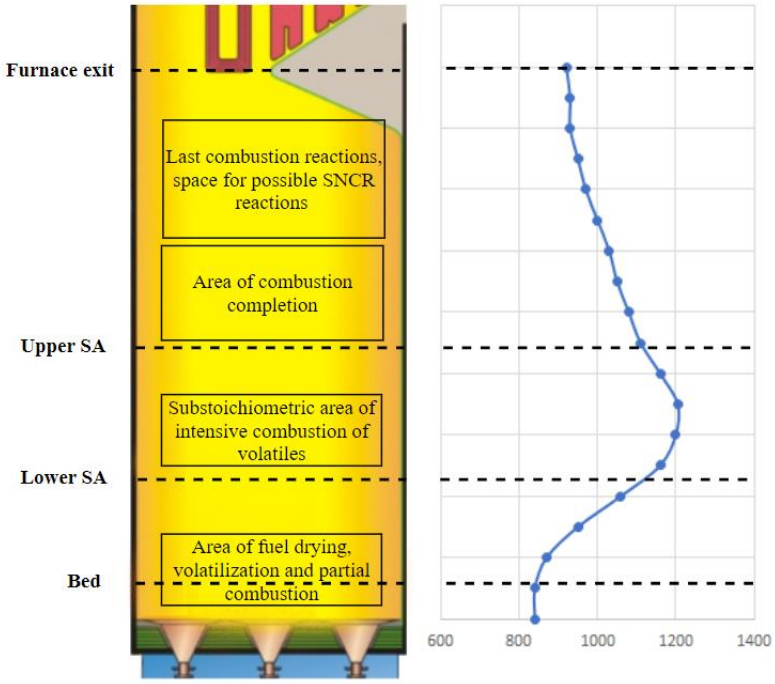

Figure 8. BFB boiler sample temperature profile (right) and rough estimation of combustion zones related to SA stages (left). Note that area over lower SA is not always sub-stoichiometric.

Stoichiometry is a concept used to describe the amount of air required for the complete combustion of a fuel in ideal conditions. Even though the absolute best combustion conditions inside any furnace are always far from optimal, stoichiometry is often used in the discussion of combustion air amounts. A typical combined rate of total airflow to the furnace is around 1.2-1.4 times the stoichiometric air amount, depending on the fuel used. Staging the air input between PA and multiple SA levels can be used to create areas where there is not enough oxygen for full combustion. For example, using sub-stoichiometric air amounts in the bed area has importance in controlling bed temperature (Basu, 2006, p. 248).

Emission requirements are one of the main incentives to consider when designing the secondary air system. Generally, if the emission requirements are strict for the boiler project in question, more effort should be put into the optimization of the SA system design. However, if the requirements are lenient, the working effort can be saved, and the air system can be simpler. The use of "secondary" emission control methods, such as a scrubber, SCR, or SNCR, always increases the capital cost of the plant. It also decreases the average availability, as the amount of equipment that can malfunction increases (Basu, 2015). Well-designed air staging is required to minimize the base level of NO_x emissions to optimize the use of secondary emission reduction techniques.

For example, waste combustion can be considered difficult in the terms of emissions. EU directive 2010/75 states strict rules for waste combustion conditions. It states that waste incineration or co-incineration plants should be able to raise flue gas temperature to 850 °C for two seconds after the last secondary air stage, during any operating conditions. The plant should include at least one load burner, which is operated with automation connected to the aforementioned flue gas temperature requirement. For hazardous wastes, that contain more than 1 % halogenated organic compounds, temperature of 1100 °C is required instead. Due to this, BFB boilers are not suitable to combust hazardous waste. Higher emphasis shall be put on the design of secondary air system for waste combustion units. This can include the use of three or more SA levels, or an otherwise more complicated design. (The European Union, 2010), (Liimatainen, 2022)

The combustion and emission-related behavior of the furnace can differ a lot during the real operating conditions compared to the estimations used during the design. To allow proper options to tune the air system during plant commissioning and operation, some staging margins must be accounted for during air system/nozzle design. For example, this could be done to allow changes between the default staging between upper- and lower SA levels or horizontally inside a single level. Margins are applied nozzle dimensioning so that the installed nozzles have enough capacity to operate with the increased flow. Some margins are also required during the fan dimensioning, to ensure that the installed fans are capable to withstand the possible increased pressure loss.

If the boiler needs to meet very strict emission requirements, more room for adjustments is required, which can be provided by using larger margins on top of the dimensioning values. Excessive use of unnecessary staging multipliers should be avoided, as it can lead

to over-dimensioning of equipment, such as the SA fan. This means that the additional maximum flow or/and pressure loss on top of the actual calculated flow results in a too large fan which then operates sub-optimally during normal operation.

5.2 Secondary air nozzle arrangement

There are technically many ways to arrange SA feeding for an air level, but the most common option is to place nozzles in two opposing rows. The overall arrangement choice is made mainly based on the boiler size class and the amount of airflow. Nozzle amounts and size is chosen case by case, again depending mainly on the parameters mentioned above. Using opposing nozzles can help to provide sufficient air coverage without having excessively high velocities. A singular feeding wall can also be sufficient for very small boilers. In some cases, the optimal choice can be to place smaller-sized nozzles opposite large ones to obtain the desired jet penetration length (1. in figure 11).

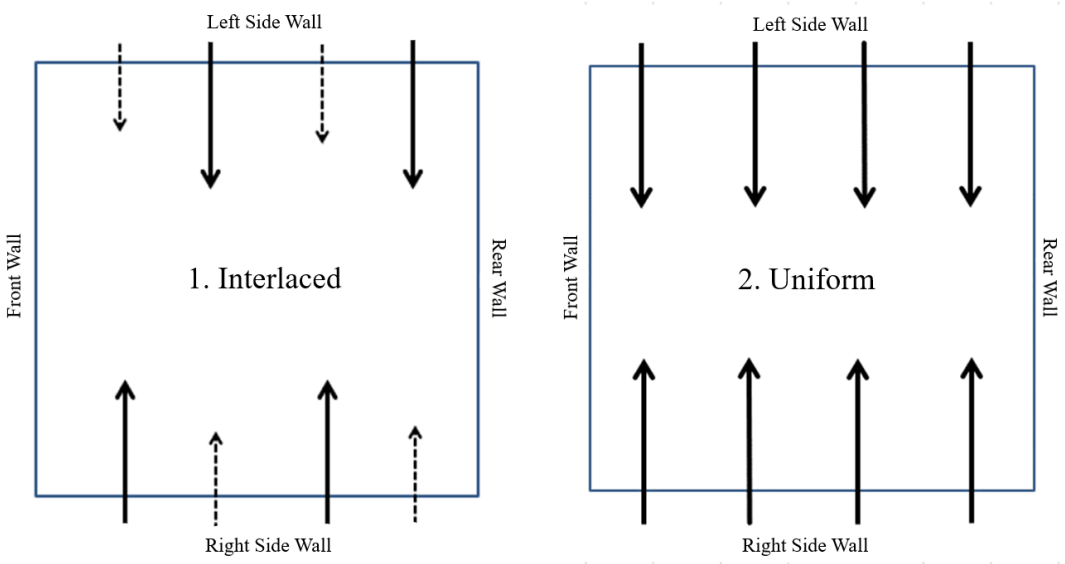

Figure 9. Example SA nozzle arrangement options for BFB boiler walls.

The vertical placing of SA stages always requires consideration case by case, even though there are some guidelines to be used. For example, SA feeding can cause disturbance to the fuel feeding, if the lowest SA level is placed too low. This must be considered especially when designing an air system for a boiler that has a main fuel consisting of fine particles (e. g. milled peat, sawdust).

5.3 Nozzle dimensioning

Good coverage of secondary air across the furnace is required to achieve the effects desired from the air staging. The number and sizes of the nozzles should be chosen case by case according to the furnace size and total airflow. As a rule of thumb, large furnaces also have large air flow rates as well. Velocity in the nozzles is a result of total volumetric air flow divided by the area of nozzles. Due to this, choosing too small or too few nozzles can result in unnecessarily high velocities. Though good penetration of the SA air jets to the middle of the furnace is strived for, too strong air jets can result also in non-uniform mixing and the development of high-temperature peak regions in the furnace.

5.3.1 Nozzle pressure loss

Nozzle pressure loss evaluation is necessary during the SA dimensioning, as it is required during fan dimensioning along with other pressure losses of the air path. It can be estimated with the following equation:

$$\Delta p = k * p_{dyn} = k * \frac{\rho v^2}{2} \tag{2}$$

where k is loss coefficient, ρ is density, and v is velocity. k accounts for combined losses resulting from the nozzle geometry and friction loss. The more complex the used nozzle geometry is, the more pressure loss it generally causes. Loss coefficient k is used to combine all geometry-related losses and friction losses. Loss-inducing elements in a typical nozzle geometry include a bend, size reduction, and outlet for example. Table values can be found for all aforementioned elements. Equation 2 is used as presented in the calculation tool developed during this work.

It’s important to consider that rise of velocity results in the rise of pressure loss. To avoid this, unnecessarily high velocities should be avoided in SA nozzles. Pressure losses are prone to rise especially in large boilers which require more jet penetration to cover the furnace and have larger air flows. To a certain extent, choosing to opt for larger nozzles can help in lowering pressure loss, as it lowers the air velocity as air volume flow stays constant.

5.3.2 Nozzle jet penetration

As mentioned above, too large nozzles can create strong jets colliding with each other which will result in airflow with high velocity in the vertical direction, turbulence, and other unwanted and hard-to-predict phenomena. Too strong and harshly colliding secondary air jets might also produce unwanted high-temperature peak regions in the middle of the furnace. Especially for one wall feeding of secondary air, too strong jets can impact the opposing wall. If particles get entrained with the jet, this can cause unexpected erosion on the wall structures. On the other hand, if the achieved penetration lengths are insufficient, the air coverage is left poor in the middle of the furnace or near the opposing wall in the case of one-wall feeding. To avoid these detriments, and to ensure a design that allows good secondary air mixing, understanding different phenomena affecting nozzle jets is very beneficial.

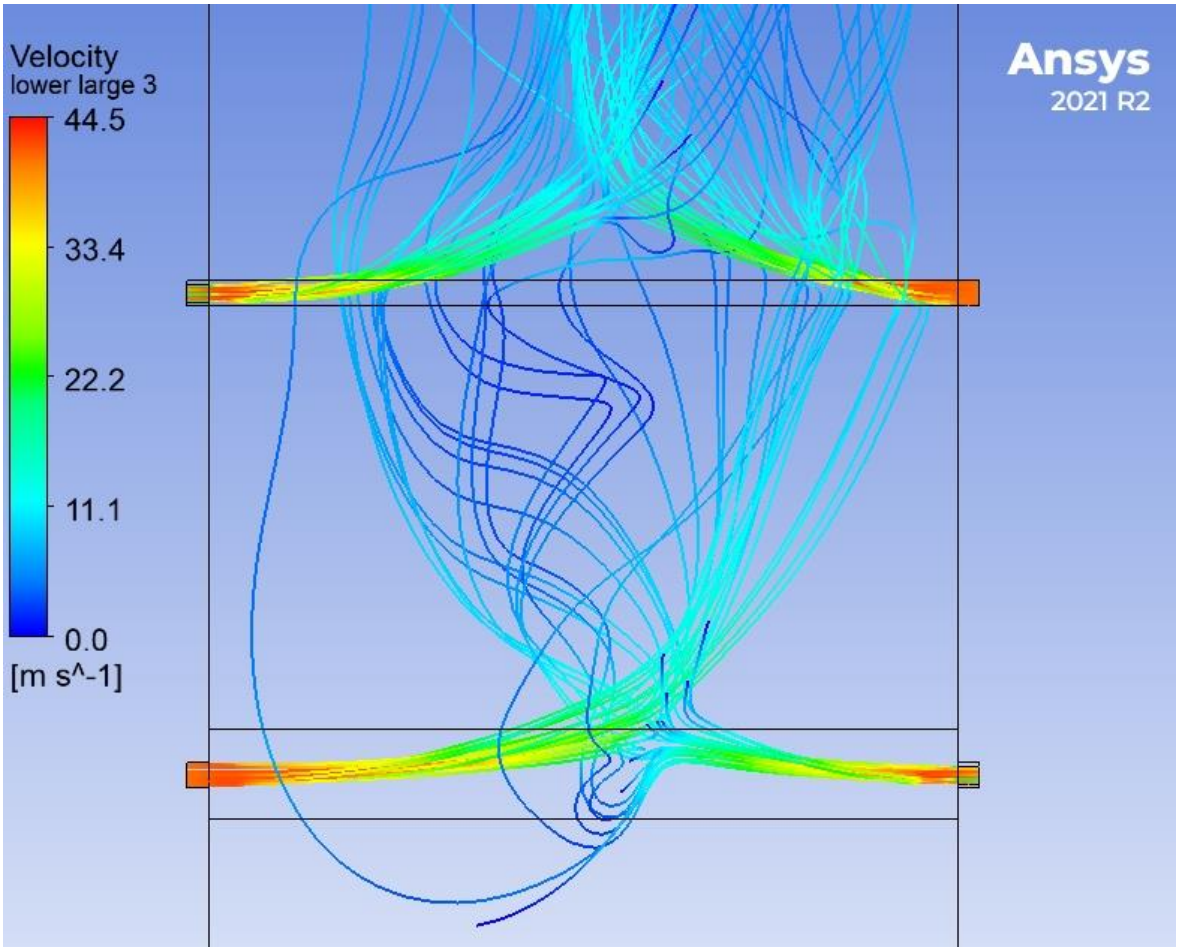

Figure 10. Upper and lower secondary air jet streamlines obtained from results of simulation of furnace gas reactions. (Adapted from SHI FW internal materials, 2022)

Figure 12 does well in illustrating the behaviour of opposing secondary air jets in the furnace freeboard. It shows both lower and upper SA stages with equal pairs of large and small nozzles. On the lower level, a larger SA nozzle is located on the right side, while on the upper level it is on the left. Opposing jets impact each other as expected, but the behaviour of the upper air level is a bit irregular, as it's harder to identify which one of the jets is stronger. However, if the velocity contours of the streamlines are observed closely, it can be seen that the right jet of the upper SA level retains more of its velocity after the jets collide.

The differing behavior of the two otherwise equal nozzle pairs can at least partly be attributed to the difference in upwards velocity. This increases the upward bending of the jets and affects the way in which they impact each other.

Jet penetration length is used to measure the distance how far into a suspension or bed a gas jet travels from a nozzle. However, it is often defined or measured differently between sources. For example, the penetration length graphs used in the previous calculation tool were made by graphically measuring a point from CFD -results, from which the air jet starts to lose velocity heavily, turn upwards and disperse. Wang et al. (2015) mention the gas volume fraction of 0.8 to measure the end of the gas jet in their study, where they researched jet penetration lengths in a simplified fluidized bed model using CFD. Hong et al. (1995) measured penetration lengths visually based on how large cavity is created in the bed by the air jet.

Estimations of jet penetration length can be used to aid in the nozzle design process to determine if the chosen nozzles and calculated air velocity lead to feasible nozzle jets with the chosen flow. Air system performance, including jet penetration lengths, can be evaluated from CFD simulations of the furnace gas reactions. However, it is time-consuming and often only feasible when a project moves forward after the bidding phase. When CFD analysis can't be performed, a faster method of estimating jet penetration lengths is required. Possible methods considered for creating a simpler evaluation tool are either generating a data set based on multiple CFD-simulations and then creating an evaluation tool based on that, or using a premade correlation found in the literature.

6 Methods for measuring jet penetration length

The understanding of factors that affect nozzle jet penetration length is crucial to successfully developing the penetration evaluation section of the calculation tool. Dawe et al. (2008) effectively compiled conclusions from different studies in their research. Nozzle and flow properties affect the penetration length; both nozzle diameter and air velocity raise jet length (Merry 1975). Of bed properties, density of the suspension, solids entrainment rate, and fluidization velocity all shorten the effective penetration length. However, at least in theory, higher fluidization velocity does not necessarily block the jet and rather increases its bending upwards. Further studies by both Zhu et. al. (2000) and Musmarra et. al. (2000) again suggested that the increased amount of solid particles in the suspension will decrease the jet penetration length. Latter of which also mentioned larger bed particle size as a reducing factor. (Dawe et al., 2008)

Jet penetration length in a fluidized bed is impacted by both properties of the airflow to the nozzle and the properties of the suspension in which it is fed. To further summarize the jet-related parameters affecting the penetration length, it is mainly dependent on the mass flow of the jet. Mass flow is dependent on gas density, nozzle diameter, and velocity. Then again, the temperature of the gas must be considered as it has relatively high impact on gas density. Overall, a larger nozzle diameter indicates more flow, thus higher penetration length when calculating with the correlations presented in this chapter.

As mentioned above, prevailing conditions in the furnace also have a large impact on the jet penetration length. These factors include suspension density and upwards (z) velocity in the freeboard at the nozzle elevation level, both of which differ greatly between bubbling and circulating fluidized beds. As known, more bed material is present at higher elevations of CFB boiler due to the considerably higher fluidization velocity. The more particles are entrained in the upwards stream of the furnace, the more suspension density rises. In BFB, the bed material mostly stays in the bed and even the lowest SA levels (at around 4 m height from the grid) are located considerably above the bed (around 1 m). At these heights, suspension density is very low.

In modern BFB boilers, secondary air nozzles are placed rows opposite of each other on the furnace walls. This inhibits the penetration length of both opposing jets as the air

streams impact each other. The size of the opposing nozzle is only roughly tied to the size to the larger “main” nozzle, and it would be hard to account for in an equation. All correlations studied in this work are made for singular jets without any opposing flow.

Implementing any of the studied correlations as a part of the calculation tool requires that all necessary parameters are possible to obtain by the user. Nozzle properties are easy to include in the calculation tool, as all required parameters are either obtained from previous calculations (air density) or calculated or chosen as a part of the dimensioning work (nozzle diameter, air velocity in the nozzle). Parameters related to the boiler operation are more problematic to calculate, namely the amount of solid particles, which is present in Merry’s and Hong’s correlations (introduced in the following chapters) as volume fraction ε. Determining an accurate ε value proved to be practically impossible in the scope of this work, thus rough estimations are used instead.

6.1 Entrainment of solids in BFB freeboard

As mentioned above, the amount and properties of the solid particles in the freeboard of the BFB have at least theoretical impact on the penetration length of the nozzle jets. However, the amount of solids present is hard to determine accurately. Bubble eruptions at the bed surface are known to be responsible for a large share of the particle entrainment in BFBs. Bubbles generated in the bed travel upwards and when they hit the bed surface, they launch particles into the freeboard. Coarse particles fall back to the bed while the finest particles continue their travel within the flue gas stream. These particles include the initial bed material, ash ,and unburned fuel particles. (Cahyadi et al., 2015)

Transport disengaging height (TDH) defines the height, over which the concentration of the particles does not meaningfully change. Below this, coarser particles that travel upwards are present, before falling back to the bed. Calculating TDH could be one way to help to determine the suspension density at the secondary air elevations. Cahyadi et al., (2015) compiled a list of 25 equations to calculate TDH which could be in theory used to support the penetration length calculations in this work. However, they mention that the correlations give very disproportionate results between each other, citing differences in TDH definitions and experimental methods as part of the reasons. Due to these uncertainties TDH calculations were not used in this work. (Cahyadi et al., 2015)

Saario, (2008) presented a correlation (originally formulated by Lewis et al., 1962) to calculate fluidized bed suspension density in his study of a CFD based model of emission formation in BFB boiler furnace. It can be seen below in equation 3

$$\rho_c = \rho_{c,o} e^{-\alpha h} \tag{3}$$

where $\rho_{c,o}$ is the density just above bed surface, α is a decay constant and h is the current elevation. α is function of particle density and value of 3.3 m^{-1} is used during the calculations below, while 400 kg/m^3 was used for $\rho_{c,o}$.

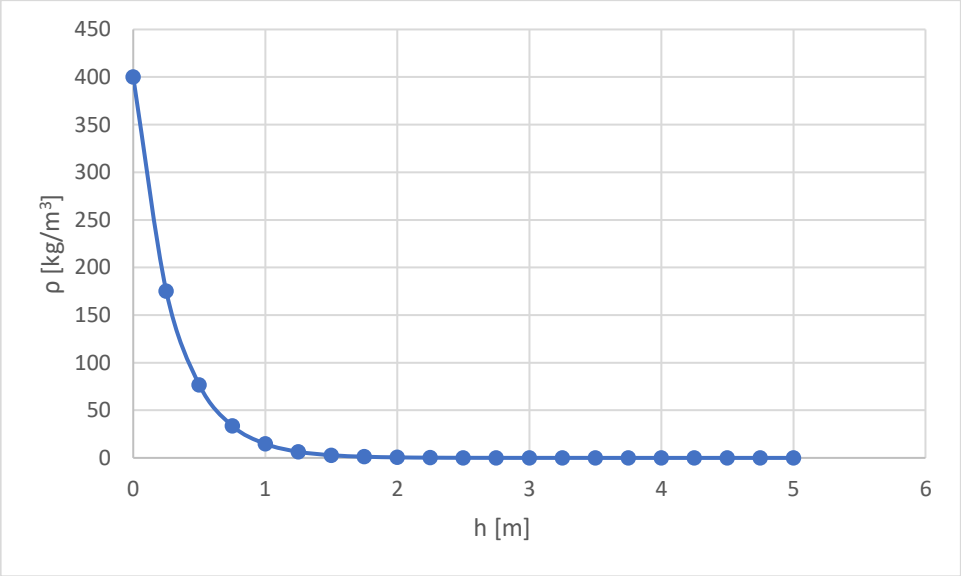

Figure 13. Suspension density calculated with equation 3 with elevation of 0-5 from bed surface.

Results of the suspension density calculation can be seen from the figure 13 and table 4. As can be seen, the density values lower rapidly towards 0 while the height rises. If considering the suspension density as the density of the gas and solids mixture in the freeboard, the lowest limit of density should be equal to the gas density. Based on this assumption the lowest values presented by equation 3 are too low compared to flue gas density (around 0.3 kg/m^3 at 900 °C). Due to this, equation 3 can't be used as full basis of the suspension density estimations in this work. The calculations further into this work use the suspension density value of around 0.55 kg/m^3. (Saario, 2008)

Table 4. Suspension density values calculated with equation 3 with an elevation of 0-3 m from the bed surface.

h [m]	$\rho_{c,o}$ [kg/m^3]
0	400.00
0.25	175.29
0.5	76.82
0.75	33.67
1	14.75
1.25	6.46
1.5	2.83
1.75	1.24
2	0.54
2.25	0.23
2.5	0.10
2.75	0.04
3	0.02

6.2 Shortcomings of experimental testing systems

A considerable effort in recent times has been made to study air jet penetration to fluidized beds, both numerically and experimentally. The varying experimental testing setups used are often simplified and downscaled systems made to recreate fluidized bed conditions seen in the chemical or energy industry. However, the systems used for the testing often do not represent the conditions of fluidized bed boilers at all. In addition to this, some otherwise insightful studies of the subject of jet penetration lengths specify on a completely different field compared to commercial energy generation, such as petrochemistry.

For example, Hong et al. (1997) presented a promising correlation for calculating jet penetration lengths (can be seen in chapter 5.3.4). However, the test system used has apparent differences compared to a commercial BFB boiler (figure 14**)**. The experimental setup consisted of a 2-D 314 x 25 mm cold fluidized bed equipped with 12 pressure measurements. The secondary air jet is fed straight into the dense part of the bed, while in a BFB boiler, the lowest secondary air stage is considerably above the bed, in the freeboard. This all indicates that the correlation presented in the paper of Hong et al. might not be efficient in predicting penetration lengths of secondary air jets in BFB boilers. It is likely that most of the correlations studied in this work are obtained in similar ways.

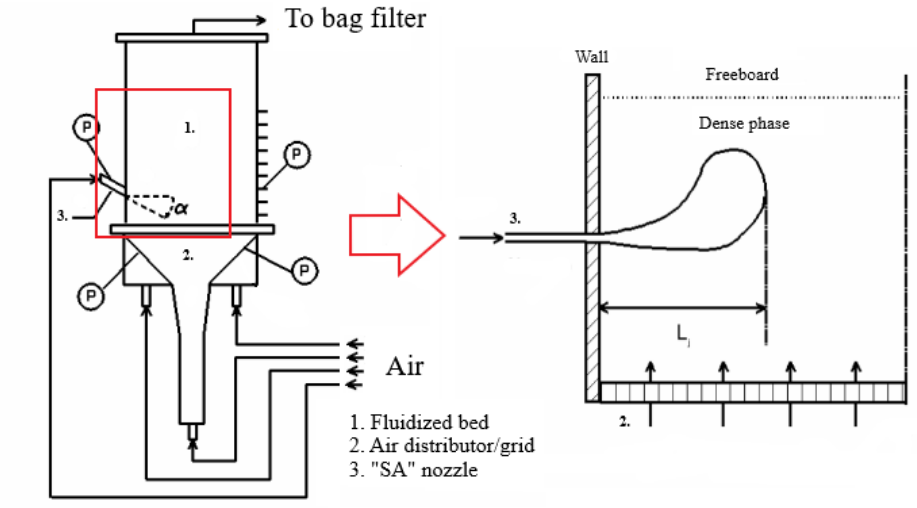

Figure 14. Schematic of experimental 2-D fluidized bed setup used by Hong et. al. to study jet penetration. (Adapted from Hong et al., 1997)

6.3 Experimental correlations for jet penetration length

Promising options to calculate jet penetration lengths found from the literature are compiled in this chapter. The usability of correlations is considered from the standpoint of BFB boilers and specifically in terms of the calculation tool developed. For example, all secondary air and FGR-related data are available in the calculation tool, but furnace conditions such as suspension density and upwards velocity are not available in the current scope of it. Studying the effect of the parameters such as bed/freeboard density could give an indication of how problematic this is and if just a universal estimation for every case could be used. The penetration length calculation is only required to give rough estimations for the nozzle design to aid in the design process.

As discussed before, the bed area is a distinctive zone with the height of 1-1.5 m from the fluidizing grid. Lower secondary air feeding elevation is often located at least 3-5 m upwards from the bottom of the grid. Only a small amount of the solid material becomes entrained off the bed into the flue gas stream, which results in the freeboard suspension density being lower than in CFB for example. Most of the correlations presented in the chapter are made to represent a completely different situation where the air jet is injected into a bed of solids. This puts the applicability of the jet penetration correlations into question, especially if they don’t include any parameters to account the fraction of solids in the medium the jet is fed to.

A correlation to calculate jet penetration lengths was presented by Savolainen and Karvinen (2001) (originally proposed by Simonen, 1999), formulated based on experimental results obtained using suspension densities from 30 – 120 kg/m^3. They concluded that the correlation would be accurate in predicting penetration lengths to dilute suspension, which could be an indication of applicability for BFB calculations. However, it must be kept in mind that the densities at BFB freeboard are noticeably lower based on the discussion in chapter 6.1. Despite this, it still has potential compared to its counterparts. Simonen's correlation can be seen in equation

$$x = 2.48\left(\frac{y}{l_m}\right)^{0.4}\left(\frac{\rho_j}{\rho_c}\right)^{0.1} l_m \tag{4}$$

where U_j is the jet velocity, ρ_j is the density of gas jet, ρ_c is the density of the suspension and l_m is characteristic length scale. The length scale is defined by the following equation

$$l_m = d_j\left(\frac{\rho_j}{\rho_c}\right)^{\frac{1}{2}}\frac{U_j}{U_c} \tag{5}$$

where U_j is jet velocity, U_c is suspension velocity, and d_j is nozzle diameter. The suspension density ρ_c seen in the equations is calculated using the following equation

$$\rho_c = (1-\varepsilon)\rho_p + \varepsilon\rho_{fb} \tag{6}$$

where ε is gas volume fraction in the freeboard, ρ_p is particle density and ρ_{fb} is gas density in the freeboard. Simonen's equation is special in the sense that it allows one to "plot" the jet and possibly study the behavior of opposing jets better. This could be beneficial as SA feeding with opposing nozzles is the most typical option for BFB units.

Merry (1971) formulated correlations to calculate both horizontal and vertical jet penetration lengths at the start of the 1970s, which are still widely referred to in studies concerning jet penetration. The equation for horizontal jets can be seen in the following equation

$$\frac{L}{d_j} = -4.5 + 5.25\left(\frac{\rho_j U_j^2}{(1-\varepsilon)\rho_p g d_p}\right)^{0.4}\left(\frac{\rho_j}{\rho_p}\right)^{0.2}\left(\frac{d_p}{d_j}\right)^{0.2} \tag{7}$$

where ρ_j gas density in the nozzle, d_j is nozzle diameter, U_j is gas velocity, ρ_p is particle density, ε is gas volume fraction and d_p is particle diameter. Note the presence of ε, which can be problematic to measure, as mentioned earlier.

Based on both experimental studies and numerical simulation of a two-dimensional fluidized bed, Hong et al. formulated a similar correlation to calculate jet penetration lengths. A major focus of their study was to develop a reliable correlation to be used for nozzles with either a downwards or upwards inclination. Along with the full correlation for inclined nozzles, they also presented a simplified version, which neglected the terms which account for feeding elevation and nozzle inclination angle. As the BFB secondary air nozzles are horizontal, the simplified version is presented below in equation

$$\frac{L}{d_j} = -3.80 + 1.89 * 10^6 \left(\frac{\rho_j U_j^2}{(1-\varepsilon)\rho_p g d_p}\right)^{0.327} * \left(\frac{\rho_j}{\rho_p}\right)^{1.974} \left(\frac{d_p}{d_j}\right)^{-0{,}040} \quad (8)$$

where symbols are same as specified earlier for Merry's correlation. The experimental study which produced the data on which the correlation is based around was discussed earlier in the chapter 6.2. The air jet is fed to a dense part of a fluidized bed which creates a visible cavity in the bed. Jet penetration length is defined as the horizontal length of this cavity. This is evidently different compared to the current definition used in the calculation tool. Defining the penetration length in BFB this way is practically impossible, as the jet cannot produce a similar cavity as it's fed to gas/solid suspension containing mostly gas. In theory, this could still be used, as gas volume fraction ε at least partly accounts for the difference between mediums the jet is fed to. How well the correlation works with very high ε values is to be determined.

Another pair of similar correlations were selected for further inspection from the study of Dawe et al. (2006). Both contain the same parameters, only with different constants. The first one presented originally by (Yates et al., 1988) is seen in equation

$$\frac{L}{d_j} = 2.8 \left(\frac{\rho_j U_j^2}{(\rho_p - \rho_j) g d_j}\right)^{0.4} \quad (9)$$

where ρ_p is particle density, ρ_j is jet density, U_j is jet velocity, g is gravitational acceleration and d_j is nozzle diameter. A similar correlation as above was presented by

Benjelloun et al., (1995). It's presented below as equation 10 with the same symbols as equation 9.

$$\frac{L}{d_j} = 5.52\left(\frac{\rho_j U_j^2}{(\rho_p - \rho_j) g d_j}\right)^{0.27} \tag{10}$$

Neither Benjelloun's nor Yates' correlation has any term to account for the amount of entrained solids in the suspension. This means that the value of the parameters would be the same for a case with a jet to a dense bed versus a case with a jet to a very diluted suspension BFB freeboard. For this reason, their applicability to BFB boiler calculations is unlikely. The last correlation to be studied is also found in the study of Dawe et al. (2006), originally presented by Zenz, (1968). The original source material was once again unable to be found. The correlation can be seen in the equation below

$$\frac{L}{d_j} = \frac{-1.48 * 0.5 \log_{10}(0.67\, \rho_j U_j^2)}{0.044} \tag{11}$$

where ρ_j is jet density, U_j is jet velocity and d_j is jet diameter. Surprisingly, the correlation does not include any parameters related to the bed or suspension into which the jet is fed into. This could indicate that perhaps the correlation is only valid for a certain range of parameters or beds/suspensions. Equation 11 is deemed unlikely to provide any meaningful results due to similar reasoning to equations 9 and 10.

6.4 Comparison calculations

The attempts made to test the applicability of any of the aforementioned correlations for SA calculations of BFB boilers are presented in this chapter. The testing calculations are done with parameters estimated to be roughly consistent with BFB boiler operation. Starting parameters can be seen in table 5.

Table 5. Initial values used in the jet penetrations correlation study.

Jet parameters			Initial values 1	Initial values 2	Initial values 3	Initial values 4
Jet density	ρ_j	kg/m^3	0.763	0.763	0.763	0.763
Jet/nozzle diameter	d_j	m	0.20	0.20	0.10	0.27
Jet velocity	U_j	m/s	40	60	50	50
Suspension parameters						
Suspension velocity	U_c	m/s	3.0	3.0	3.0	3.0
Gas volume fraction	ε	-	0.9999	0.9999	0.9999	0.9999
Freeboard gas density	ρ_{fb}	kg/m^3	0.30	0.30	0.30	0.30
Solid particle density	ρ_p	kg/m^3	2500	2500	2500	2500
Suspension density	ρ_c	kg/m^3	0.550	0.550	0.550	0.550
Solid particle diameter	d_p	m	0.0005	0.0005	0.0005	0.0005

Scala et al. (2013) presented three different density definitions: material density, particle density, and bulk density. Material density can be defined as the true density of the material, even excluding the internal pores of the particle. Particle density on the other hand includes the possible internal pores that can be present in the subjected particle. For sand, material density is only slightly higher than particle density, as sand particles are not very porous. Bulk density is defined as the mass of particles divided by the occupied volume, taking the voids between particles into account. Suspension density in this work refers to the average density of the mixture of gas and solids in the furnace freeboard. Typical particle density for silica sand is often around 2400-2600 kg/m^3 and Scala et al. mentioned 2600 kg/m^3 as an example of material density. In this study, 2500 kg/m^3 particle density is used to represent bed material.

A typical particle diameter for BFB boiler bed material is at the lower end of 0.5-2 mm as mentioned before in chapter 2 (Vakkilainen, 2016). 0.5 mm is used as the average in the calculations, as smaller particles are more likely to be entrained. Possible SA jet velocities at the nozzle range broadly from 30-90 m/s and tested velocities are chosen from this range. Nozzle diameters are also chosen based on the range of typical sizes. Temperatures in the freeboard can vary at least between 800-1200 °C, which brings the gas density low. A rough approximation of 0.3 kg/m^3 is used in the testing, but an even lower value could be used. These values are meant to represent conditions at the lower SA levels, at elevations of 3-4 m from the grid 0-level. ε value of 0.9999 is used, roughly on the basis

that it results in a suspension density of 0.550 kg/m^3, which in turn somewhat matches with the suspension densities discussed in chapter 6.1.

The summary of the correlations used in the testing can be seen in table 6. The testing consisted of two parts:

1. Initial calculations to determine if any of the correlations show promise of being applicable for very a diluted suspension
2. Further calculations with selected correlations to determine the impact of important parameters, such as U_j and U_c.

It must be noted that the used values are uncertain at best, especially the values of particle diameter and gas volume fraction. Results presented in this work should only be used as indicative values.

Table 6. Summary of studied correlations. (Adapted from Dawe et al., 2008)

Author	Correlation
1. Zenz, (1968)	$\frac{L}{d_j} = \frac{-1.48 * 0.5 \log_{10}(0.67\,\rho_j U_j^2)}{0.044}$
2. Merry, (1971)	$\frac{L}{d_j} = -4.5 + 5.25\left(\frac{\rho_j U_j^2}{(1-\varepsilon)\rho_p g d_p}\right)^{0.4}\left(\frac{\rho_j}{\rho_p}\right)^{0.2}\left(\frac{d_p}{d_j}\right)^{0.2}$
3. Hong et al., (1997)	$\frac{L}{d_j} = -3.80 + 1.89 * 10^6\left(\frac{\rho_j U_j^2}{(1-\varepsilon)\rho_p g d_p}\right)^{0.327} * \left(\frac{\rho_j}{\rho_p}\right)^{1.974}\left(\frac{d_p}{d_j}\right)^{-0{,}040}$
4. Yates et al., (1988)	$\frac{L}{d_j} = 2.8\left(\frac{\rho_j U_j^2}{(\rho_p - \rho_j) g d_j}\right)^{0.4}$
5. Benjelloun et al., (1995)	$\frac{L}{d_j} = 5.52\left(\frac{\rho_j U_j^2}{(\rho_p - \rho_j) g d_j}\right)^{0.27}$
6. Simonen, (1999)	$x = 2.48\left(\frac{y}{l_m}\right)^{0.4}\left(\frac{\rho_j}{\rho_c}\right)^{0.1} l_m, \qquad l_m = d_j\left(\frac{\rho_j}{\rho_c}\right)^{\frac{1}{2}}\frac{U_j}{U_c}$

6.4.1 Results of initial calculations

The results from first round of the calculations can be seen in the table below. Main goal was to determine which correlations should be included in further testing. Simonen's correlation is treated separately of others.

Table 7. Jet penetration length L [m] calculated with correlations 1-5. Plausible values are bolded.

	Initial values 1	Initial values 2	Initial values 3	Initial values 4
1. Zenz, (1968)	-0,107	-0,011	0,017	0,045
2. Merry, (1971)	14,837	20,867	10,355	22,702
3. Hong et al., (1997)	**4,293**	**5,827**	**2,463**	**6,962**
4. Yates et al., (1988)	0,321	0,444	0,253	0,460
5. Benjelloun et al., (1995)	0,758	0,944	0,516	1,065

Penetration lengths (L) seen in the above table are all implausibly small for correlations 1, 4, and 5. This confirms the assumption that the inclusion of parameters to account for the rate of solids in the suspension/bed is necessary to calculate with very dilute suspension (BFB freeboard). One possibility is that the density in correlations 3 and 4 should be bulk or suspension density that would account the gas fraction into account, but this can't be confirmed due to the lack of original sources. Correlations 1, 4, and 5 are excluded from further calculations.

Merry's correlation (2) produces unrealistically high values with all 4 sets of initial values and is also written off from further calculations. Correlation 3 (Hong et al.) is the most promising one, as it produces values much more realistic in comparison to other tested correlations. It's also interesting that correlation 3 produces seemingly too small values compared to correlation 2, even though they are both written similarly with the same parameters.

The results of initial calculations with Simonen's correlation (6) can be seen in figure 15. Presentation is different compared to the other correlations due to the different type of the equation and the nozzle jet is calculated with y values from 0 to 2.0 m with a step of 0.01. As mentioned before, it works differently compared to the other studies as it rather plots the jet instead of giving a clear penetration length. While there is no clear definition set for L in this case, such as a certain y value, the values seem to be very high. For example, using the starting values 4 results in a jet that reaches 20 m in length before rising 0.5 m, which is completely implausible.

It still could be valuable to study Simonen's equation. If suspension-related parameters that would make it accurately represent jets in BFB freeboard could be found, it could be a good way to estimate behaviour of opposing jets. Even though this wouldn't lead to the most scientifically valid results, it still could be used as an engineering tool if the results agree with reality.

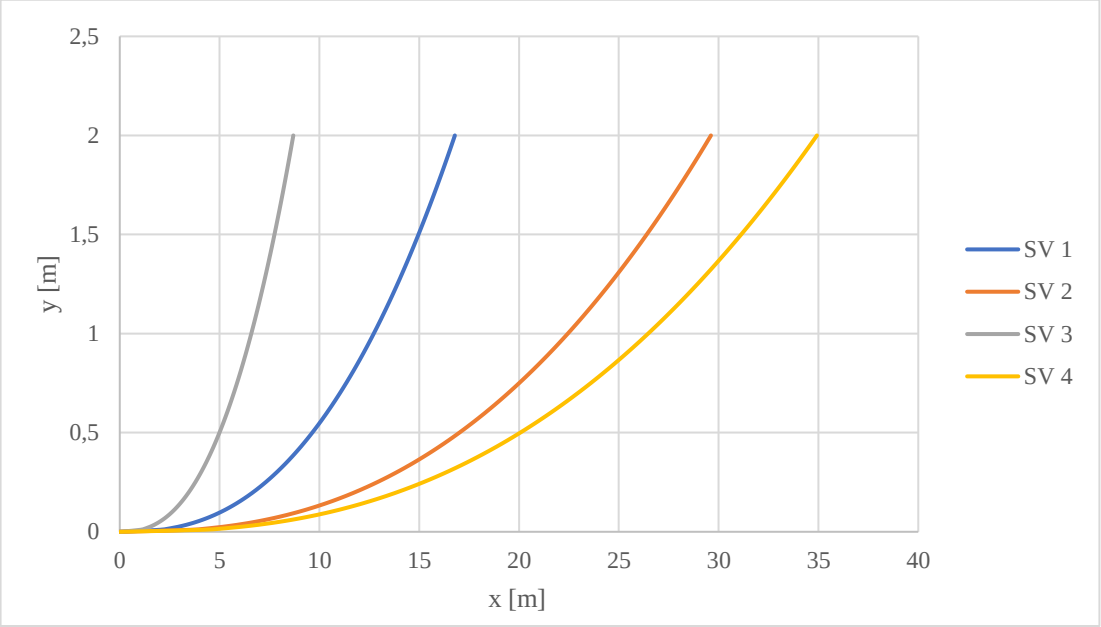

Figure 15. Initial results for Simonen's correlation. x values are unreasonably high.

6.4.2 Results of further calculations

Results obtained from further calculations with correlation 3 (Hong et al., 1997) can be found in figure 16. Penetration length *L* is calculated for 4 nozzle diameters from 70 to 280 mm and for U_j 30 to 90 m/s. Otherwise results in figure 16 are calculated using starting values 1. The slope of the graphs can be seen to increase corresponding to an increase in nozzle diameter, as it should. It must be noted that there is no clear comparison point to present with the data and they are roughly compared to nozzle sizes and velocities seen in reference boilers used in this work. However, they most often contain SA feeding with opposing nozzles, while the results are meant to represent a case without them. With that kept in mind, the values seem quite realistic, to the point that correlation 3 could be considered, especially to evaluate singular jets.

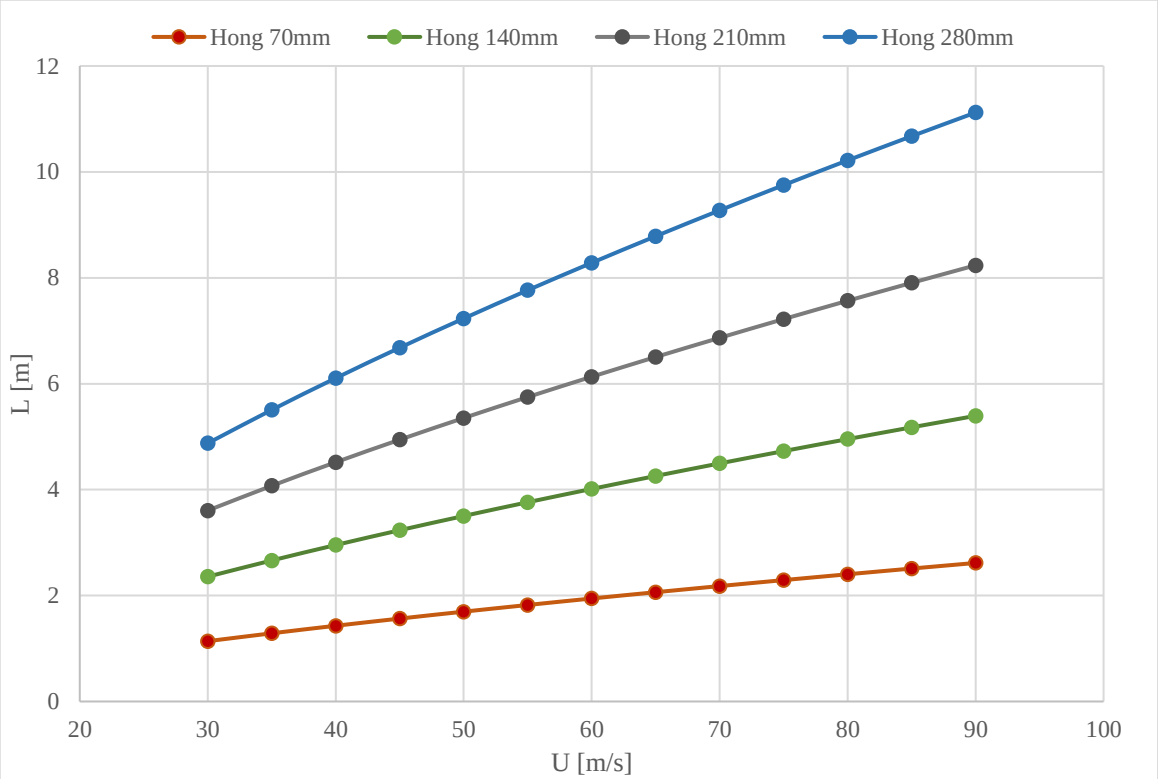

Figure 16. Jet penetration lengths calculated with the correlation 3.

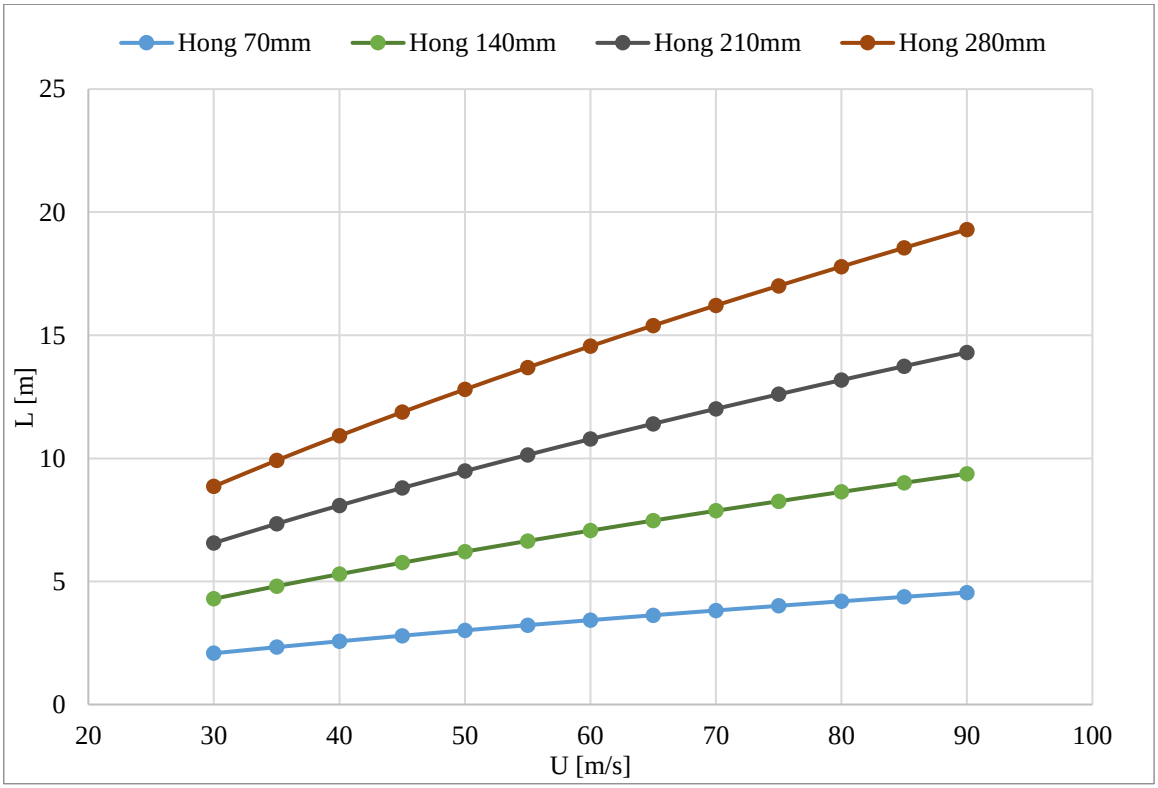

Figure 17. Results with particle density of 2000 kg/m^3, that resulted in suspension density of 0.500 kg/m^3 (with otherwise same starting values).

When comparing the results in figures 16 and 17 between each other, it can be immediately noted that Hong et al.'s correlation reacts strongly to the change in particle density. This is interesting, as the suspension density changed only a small amount. Even though suspension density is not included in the equation as a parameter, ideally the correlation should behave proportionally to the change of it.

To further validate Hong et al.'s correlation to be used during the nozzle dimensioning, CFD simulations with one wall feeding of SA should be conducted to provide a comparison point. In terms of the developed calculation tool, there is currently no good method to evaluate penetration lengths for one-wall feed cases. This could be a good area to focus on for further studies of the subject, even though cases with one feeding wall aren't the most common option.

Starting values were changed a bit for further calculations with Simonen's correlation. The gas volume fraction was lowered to 0.999, considerably raising the suspension density. Even though the values are most likely not very realistic, using them seemed to provide results that agree with their comparison points considerably better. Other parameters, such as suspension velocity and nozzle sizes were changed to match their comparison points specified further in the text.

Table 8. Values used for further calculations with Simonen's correlation. (Figures 18 and 19)

			Large BFB		Medium BFB	
Jet parameters			Lower (large pair)	Upper (large pair)	Lower (large)	Lower (small)
Jet density	ρ_j	kg/m^3	0.763	0.763	0.870	0.870
Jet/nozzle diameter	d_j	m	0.27	0.27	0.27	0.17
Jet velocity	U_j	m/s	45	45	32	32
Suspension parameters						
Suspension velocity	U_c	m/s	2.6	4.0	2.6	2.6
Gas volume fraction	ε	-	0.999	0.999	0.999	0.999
Freeboard gas density	ρ_{fb}	kg/m^3	0.28	0.28	0.26	0.26
Solid particle density	ρ_p	kg/m^3	2500	2500	2500	2500
Suspension density	ρ_c	kg/m^3	2.780	2.780	2.760	2.760
Other parameters						
Distance between nozzles	-	m	10	10	6.8	6.8

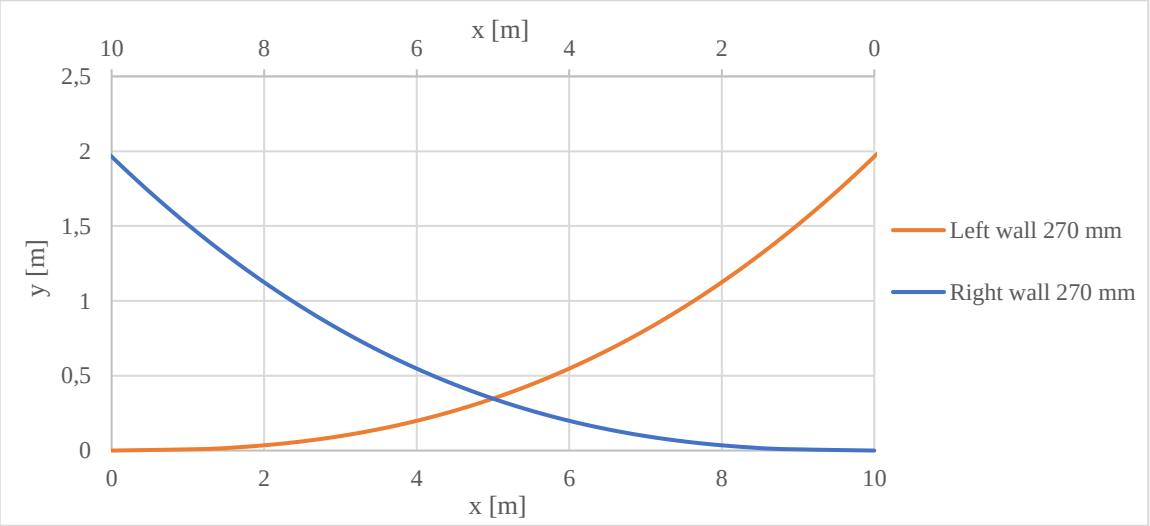

Figure 18. Results of Simonen's correlation with values of large BFB boiler lower SA level. The distance between nozzles is 10 m. Note that the used values are from table 8.

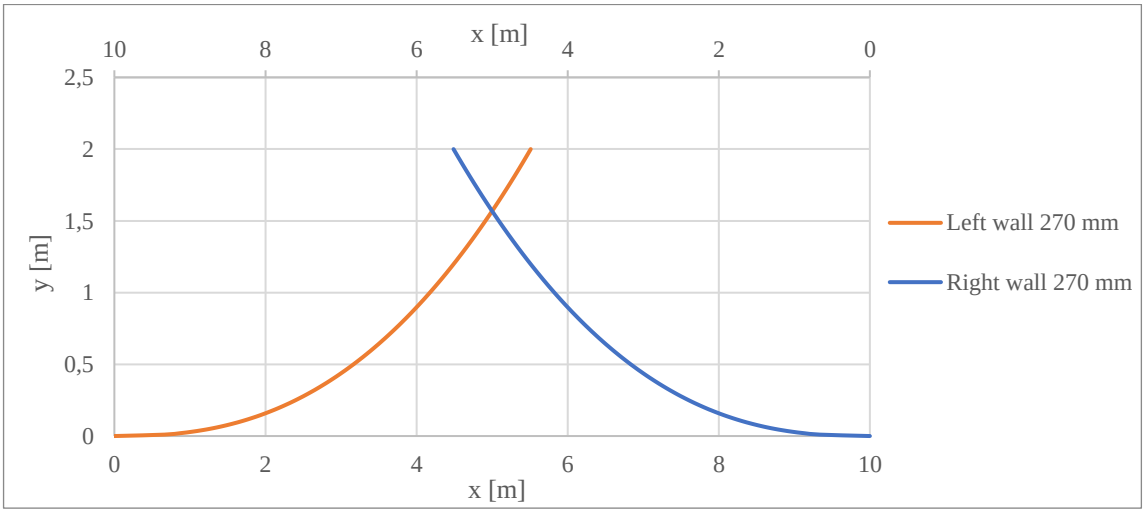

Figure 19. Results of Simonen's correlation with values of large BFB boiler upper SA level. Note that the used values are from table 8.

Based on a comparison between figures 18 and 19, results obtained with Simonen's correlation seem to react very heavily to the increase of upwards velocity in the freeboard. The collision height differs over two meters between the two figures. The CFD analysis of the boiler on which the "large boiler" -values are based was not available, which limits the analysis to more broad level. The values presented in both figures are still at least relatively realistic, which makes it a promising option for further studies. It must also be noted that the same suspension values were used for lower and upper SA. If there ever would be such

high suspension density values that are shown in the table, they should be present only in the lower parts of the freeboard, not in the upper SA elevations.

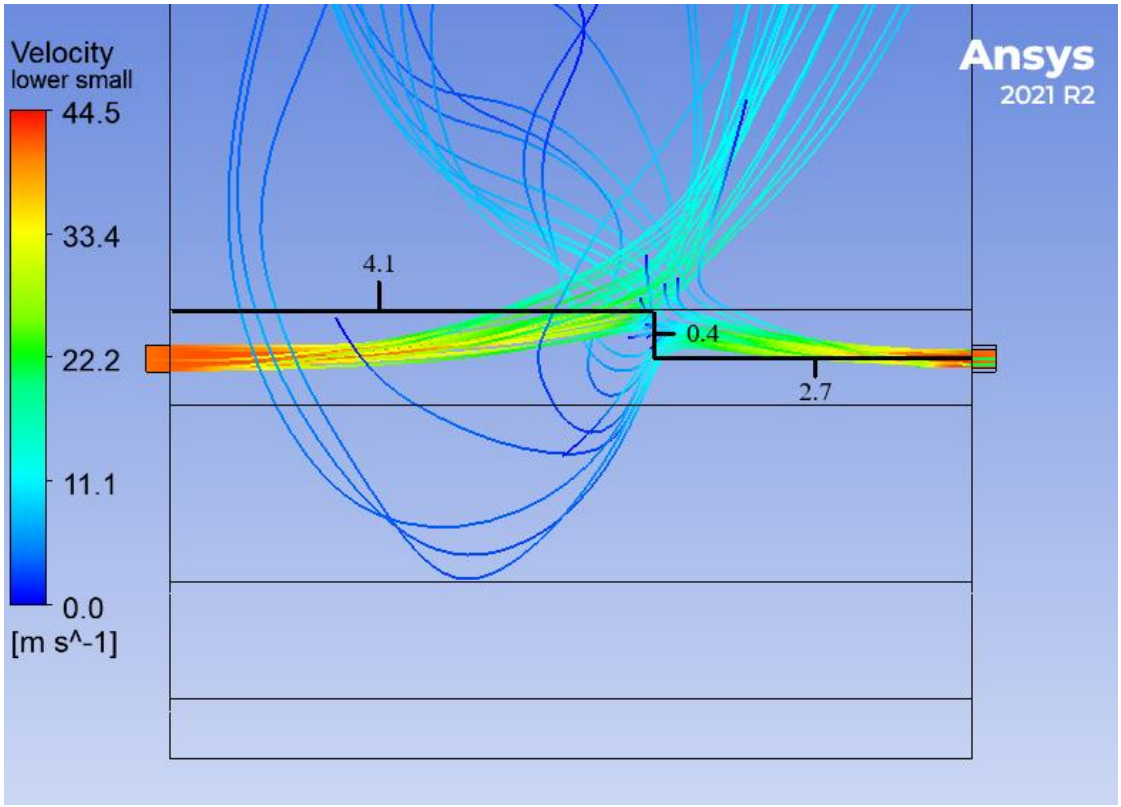

Figure 20. Lower SA jet streamlines with distances measured in metres.

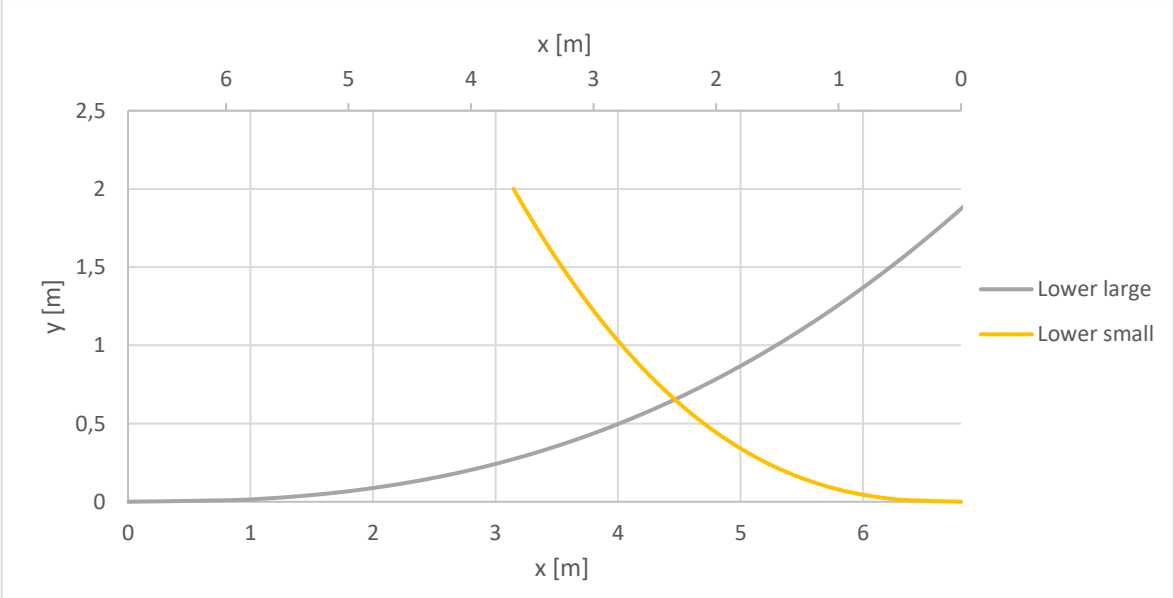

Figure 21. Results of Simonen's correlation with values of a medium sized BFB boiler lower SA level. The distance between nozzles is 6.8 m.

Figure 21 is obtained with Simonen's correlation using values comparable to values found in the CFD results, from which figure 20 is obtained. If the penetration length is defined as the interception point of the two jet penetration graphs, they can be compared. Simonen's correlation resulted in a longer jet from the large nozzle and the jets curve upwards more heavily. Results are still surprisingly close and again could indicate that the correlation is worth committing time for further testing. However, there are too many uncertainties, especially in the choice of suspension density that further analysis would be required to use it in the final calculation tool.

A way to use the correlation in the nozzle dimensioning process would be to assign limits for the collision height for both air jets. For example, if the preferred collision height would be assigned to 0.5 m for lower SA and to 1.0 m for upper SA user of the calculation tool could then choose nozzle sizes according to the limits. This would require further testing and conversations with experts to determine the correct limits. One way to validate this as the dimensioning method could be re-calculating older boilers with the calculation tool and comparing results to see if the use of Simonen's correlation would lead to similar results in terms of nozzle dimensioning.

7 Secondary air nozzle calculation tool

Performance calculations are used for each boiler delivered by SFW both during the proposal stage and the project execution. Calculations of the proposal stage are used as a basis for pricing. They are required for most major concepts or components required, for example, thermal dimensioning requires calculation for all major heat transfer surfaces based on the requirements set by the customer. These include especially the used fuels and requirements for the produced steam.

For proposals and projects alike, Sumitomo SHI FW uses its own software to create a performance calculation model of the boiler, which contains energy and mass balances and general process data including steam, air, and flue gas parameters. Data from the boiler model is used as a design basis for the dimensioning of individual components and sub-systems such as fans, the fluidization grid or the secondary air nozzles. The design and dimensioning work for them is done by a set of other calculation tools. Developing a new Excel-based calculation tool, particularly for the secondary air nozzle calculations was the main goal of this thesis.

As mentioned above, the SA calculation tool presented in this chapter is used to assist in dimensioning and design calculations during the design of BFB boilers in both proposal and project stages. The output of the tool is compiled on a so-called CI-sheet, which includes the most important results to be used further in other tools. One example of this would be the nozzle pressure loss, which is then used for SA fan dimensioning.

7.1 Requirements

Features of the dimensioning tool can be divided to fundamental and experimental features. Fundamental features represent features that are used during a more standard biomass BFB project, whereas experimental features might be only required during the design of more specialized boilers. Fundamental features to be used in all calculations include assigning standard air level configuration, designing nozzles (diameter and velocity), and calculating nozzle pressure loss for fan dimensioning. More experimental features include for example an option to calculate with flue gas recirculation fed to SA stages and inputs for more advanced SA configurations.

The following goals were set for the calculation tool development:

- clearer and more intuitive design while retaining all features of former similar tools
- reduced ability to make unforced errors by stricter input options and better guidance
- developing pre-existing features further and implementing new additional features for example:
    - better tool to study nozzle jet penetration
    - more advanced options to calculate with separate FGR nozzle levels.

The calculation tool requires inputs of air and FGR properties, furnace dimensions and arrangement choices to provide a concluding summary of the arrangement design, and nozzle properties, such as nozzle pressure loss and volume flow. A schematic of the inputs and outputs of the tool can be seen in figure below.

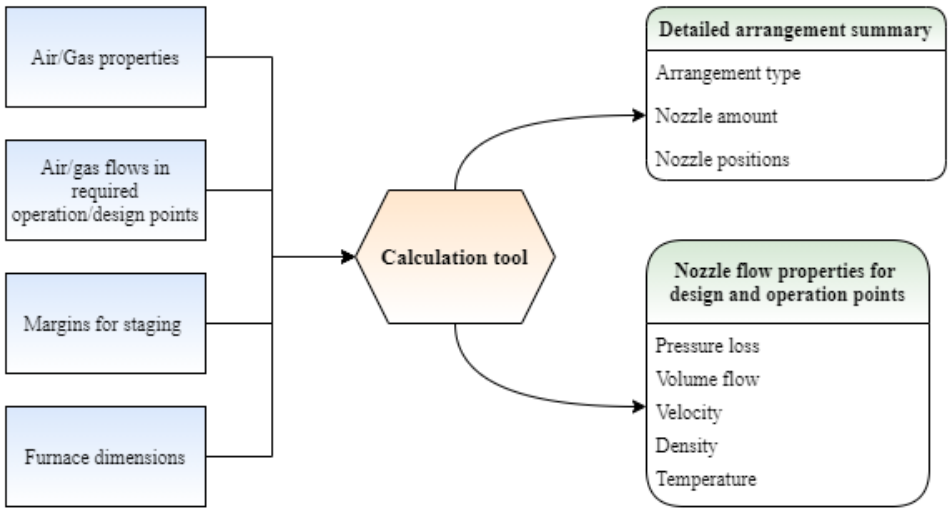

Figure 22. The inputs and outputs of the calculation tool.

The most important information required as the output of the calculation tool for further calculations is the following:

- Secondary air layout, nozzle arrangement, and amount of stages
- Required air flow rates for at least one typical operation point in addition to maximum and minimum SA flow cases

- Nozzle sizing and amount
- Nozzle pressure loss and air velocity in the nozzles.

7.2 Calculation procedure

The calculation template is split to three parts: “arrangement selection”, “secondary air flow and properties”, and “final nozzle calculations”. Even though the gas pressure in the nozzles is calculated iteratively based on the pressure loss that is a result of the calculation, the aim is for the calculation to flow linearly from each sheet to another.

7.2.1 Arrangement selection & nozzle placement

Global inputs for the whole calculation tool consist of furnace dimensions (depth, width, and height), wall tube spacing and ambient pressure, and freeboard pressure. Tube spacing is relevant as boiler walls consist of tube membrane. The tool uses the number of tubes between each nozzle as input value to space nozzles evenly to walls.

The arrangement section of the tool allows the selection of nozzle arrangement, elevation levels, nozzle amount, and positioning. The most important guideline is to position nozzles correctly so that the last nozzle of the row is not too close to the wall, while horizontal distances between nozzles stay optimal. The arrangement of nozzles is compiled into a summary table as seen in the table below. Similar options and tables are included for possible feeding levels with FGR feeding. It can be either mixed in the SA flow or to be fed to its own feeding levels.

Table 4. Sample secondary air arrangement. Interlaced is a SA arrangement option in the tool.

	Lower SA		Upper SA		Tertiary	
	Arrangement	Elevation	Arrangement	Elevation	Arrangement	Elevation
Side walls	**Interlaced**	**4000**	**Interlaced**	**7000**	n/a	n/a
Front wall	n/a	n/a	n/a	n/a	n/a	n/a
Rear wall	n/a	n/a	n/a	n/a	n/a	n/a

7.2.2 Secondary air flow & properties

To successfully obtain wanted results such as nozzle air pressure loss and velocity, air properties must be brought into the tool. Equations presented in this chapter also contain parameters to account for possible FGR feeding. However, in the most typical designs,

FGR to secondary air is not used, and the corresponding terms cancel out. The main inputs for both air and FGR are temperature, density, and pressure. Ideal gas law is used to calculate with these values, presented in the equation below

$$pV = mR_sT \tag{12}$$

$$\rho = \frac{p}{R_sT} \tag{12}$$

where p is pressure, V is volume, m is mass, R_s is specific gas constant, T is temperature and ρ is density. The nominal density of air is presented in certain standard conditions (1.01325 bar, 0 °C), accounting for air humidity in the location the boiler is to be constructed. This value is used to approximate actual density using the ideal gas law

$$\rho_{2,abs} = \rho_{1,NTP} * \frac{p_2 T_{1,NTP}}{T_2 p_{1,NTP}} \tag{11}$$

where ρ is density, T is temperature, p is pressure and the subscript NTP accounts for standard conditions specified above. Notable is that humidity is approximated to stay equal, which in turn makes universal gas constant to stay equal and cancel out. To obtain an approximation of air/gas pressure in the nozzles atmospheric pressure added to the average of pressure loss between air levels is used, as seen in equation

$$p_{mix} = p_{fb} + \Delta p_{nozzles} \tag{13}$$

where $\Delta p_{nozzles}$ is nozzle pressure loss and p_{fb} is the pressure of the freeboard at the current SA elevation. Air/gas pressure is calculated with an iteration loop as the nozzle pressure loss values are one of the end products of the calculation. After this, air flows for wanted load cases are input, and staging margins specified before are applied. Typical load cases that are calculated are worst case flow, flow at main guaranteed operation point (both with and without staging) and minimum flow. The template offers the user an option to input additional custom flow/load case to be calculated for informational purposes. Minimum values for each air level are determined based on set value for minimum velocity, which should be maintained even at part-load operation to provide cooling in the nozzles.

After the first property calculations, flow-related parameters need to be calculated separately for each wall and feeding level. The nominal and actual density are known

separately for both air and FGR, but the actual density of the gas is required for further calculations. Required to obtain actual density through the ideal gas law, the average temperature of the SA mixture is calculated using equation 14 (typically only air is present).

$$T_{mix} = \frac{T_{air} * q_{m,air} + T_{FGR} * q_{m,FGR}}{q_{m,tot}} \tag{14}$$

After the temperature of the gas is obtained, absolute density can be calculated using equation 15. It is required later during the pressure loss calculations.

$$\rho_{mix,abs} = \rho_{mix,NTP} * \frac{p_{mix,abs} T_{mix,NTP}}{T_{mix,abs} p_{mix,NTP}} \tag{15}$$

Gas velocity in nozzles can be calculated later if actual gas volumetric flow rate is known. Absolute volumetric flow rate of the gas is obtained using the equation below.

$$q_{v,mix} = \frac{q_{v,air} \rho_{air,NTP}}{\rho_{air,abs}} + \frac{q_{v,FGR} \rho_{FGR,NTP}}{\rho_{FGR,abs}} \tag{16}$$

7.2.3 Nozzle diameter input and results

After required parameters for the air flow are calculated the nozzle diameters need to be assigned. This has available inputs for each wall between all air stages, including possible FGR nozzle rows. When nozzle diameters are known, it allows to calculate total area of nozzles for each feeding wall. As total air/gas flow to that wall is known, velocities can be calculated by following equation

$$v = \frac{q_{v,mix}}{A_{nozzles}} \tag{17}$$

where $A_{nozzles}$ is total area of nozzle openings on one wall for specific stage. After velocity is calculated, pressure loss is calculated using equation 2. Pressure loss is also calculated for total of all nozzles on one wall for single air stage similarly to velocity.

$$\Delta p_{nozzles} = k * \frac{\rho v^2}{2} \tag{2}$$

Equation 2 is first introduced in chapter 5.3.1 that also contains further discussion of the parameters used.

7.2.4 Jet penetration evaluation

The jet penetration section used in the final calculation tool was decided to be done based on data gathered from old jet penetration studies instead of any of the correlations tested in this work, as none of them were proven to be applicable. The old method was based on a set of graphs (example in figure 23) which illustrated penetration lengths in the function of velocity for different nozzles. This posed problems, especially in situations where the currently chosen nozzle diameter was not available in the graph. Visually interpolating between curves is always prone to human error.

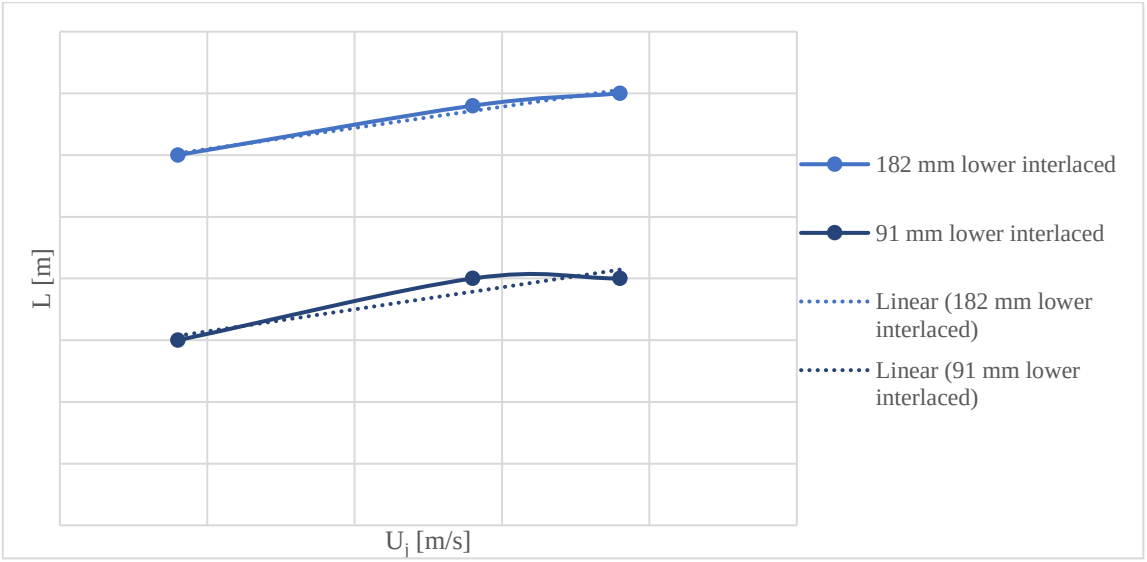

Figure 23. Example of jet penetration length graphs for two example nozzle sizes. Axis values are hidden to preserve confidential information.

The updated penetration length measurement method used in the calculation tool is based on a further developed version of the old dataset. Equations were then obtained for each curve with velocity as a variable, as shown in figure 23. This allowed us to slightly smooth the possible measurement errors in the data. Having equations for multiple nozzle sizes allows the creation of penetration length equations with nozzle size as a variable, one equation for each velocity value. This process allowed us to overcome the fact that the used dataset is lacking enough nozzle sizes to cover the required range of possibilities.

The tool requires inputs for the nozzle sizes and gas velocity. After the required inputs are set, the tool plots a figure interchangeable with the one seen below (figure 24) and calculates if the nozzles are correct based on the wall length determined by the used feeding walls. If the jet penetration length does not match the furnace dimensions, the nozzle sizes shall be changed accordingly. Penetration length is then calculated again to test the nozzles with new velocity. After good nozzle sizes are found, the calculated data is exported to further use.

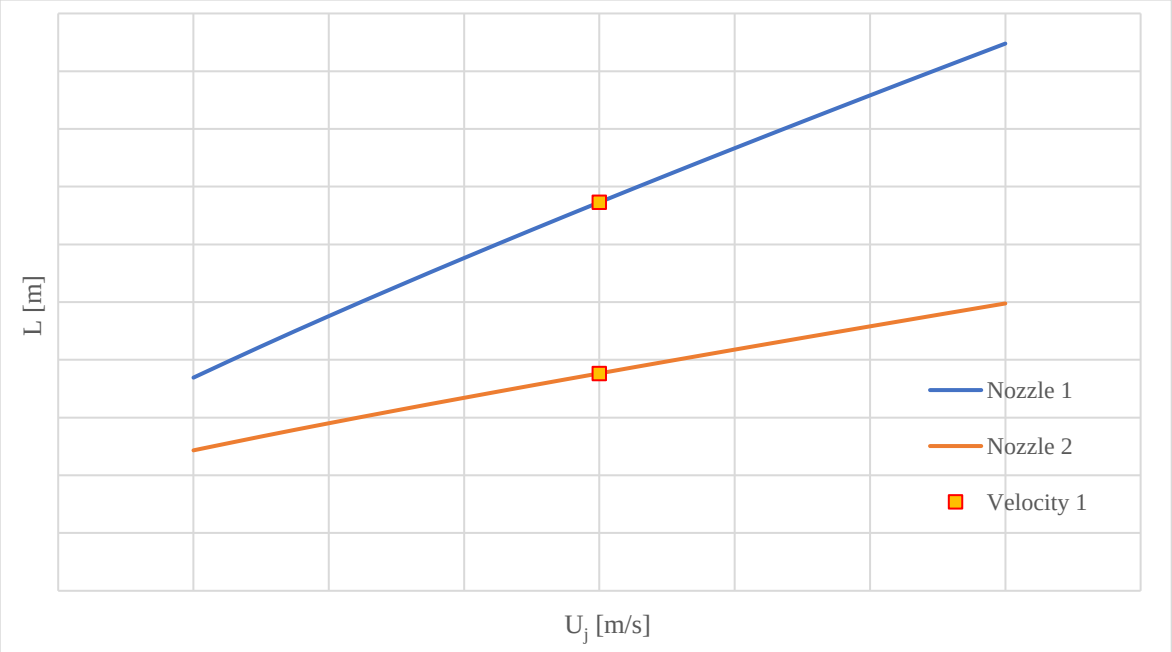

Figure 24. Example figure provided by the penetration length evaluation tool. Axis values and nozzle sizes are hidden to preserve confidential information.

7.3 Discussion of results & future improvements

Overall goals for the calculation tool development were achieved. Both usability and functionality were improved. The goals set for the jet penetration length evaluation tool development were also met, even though none of the studied correlations were used. The current evaluation method can account for all typical nozzle sizes and velocities, and it is able to automatically illustrate the results. The final calculation tool was successfully used for SA calculations of the ongoing BFB boiler proposal for an over 200 MW_{th} plant, planned for combustion forest industry residues and water treatment sludge.

Better guidance for the tool was achieved by writing a comprehensive guide to accompany the calculation tool. It is located on its own sheet with clear sections corresponding to

different sections of the tool. This allows the user to easily search the topic that is currently causing issues. Example figures of some of the most important concepts and most confusing aspects of the tool were included for clarity. To reduce human error, inputs were limited to predetermined choices whenever possible.

The ability of the tool to account for more advanced design choices was improved by adding the ability to freely implement the flue gas recirculation to be mixed to any of the three secondary air stages. The improved ability to assign flow amounts freely for different walls inside one SA level was created to support the possibility of using more unorthodox nozzle configurations in the future. Simple VBA (Visual Basic for Applications) programming was implemented to hide unused sections of the tool, which allows to preserve clarity while introducing new features.

However, the jet penetration evaluation method still has some limitations, even though progress was indubitably made. There were practically no available data from other than cases with opposing nozzles. Thus, the use of it for cases with one feeding wall is questionable. Also, the nozzle pairing used in the calculation might not be the same that was used to obtain the data the tool is based on. This naturally inhibits the accuracy of the results, as the size and velocity of the opposing nozzle have a large effect on the jet behavior. It also does not account for the density of the SA, which can differ case by case based on the temperature of the air. However, the resulting tool was deemed to be accurate enough to act as a basis of the nozzle design and the goals for the development were met.

The use of the correlations studied in this work could, at least theoretically, help to circumvent the issues mentioned above. Simonen’s correlation could be used to plot two nozzles simultaneously and the Hong et al.’s correlation could be used to evaluate possible cases with only one feeding wall. Even though they couldn’t be properly validated to be used in the calculation tool, the basis for possible future implementation has been made.

Implementing the use of a material property library to obtain air properties could be done in the future to improve the accuracy of the results. Currently, the air and gas parameters are calculated using the ideal gas law. The amount of error resulting from this compared to the use of property functions is currently unclear, but it could be worth studying in the future.

8 Conclusions

During this thesis, an Excel calculation tool was developed for the use of Sumitomo SHI FW to dimension BFB boiler secondary air nozzles. Another major goal was to develop a new method to evaluate secondary air jets in the furnace freeboard. In support of the calculation tool development, the essential theory of BFB boilers was studied with an emphasis towards air systems.

A well-designed combustion air system is the key to reaching required emission limits with the lowest number of additional emission removal systems possible. It is necessary to achieve stable combustion of difficult fuels and overall efficient furnace operation. An insufficient combustion air system can result in problems during plant commissioning, which in extreme cases can lead to delays and significant cost increases.

An effort was made to test 6 available penetration length correlations found in scientific literature to identify which of them could be used with parameters consistent with the conditions of a BFB furnace freeboard. Accurately evaluating the suspension density and particle entrainment in the freeboard proved difficult, which led to rough estimations being used during the calculations. Based on the results of the study, equations proposed by Hong et al. (1997) and Simonen (1999) showed some promise for this purpose, while the other 4 correlations were deemed unusable. Three of the other correlations tested were written in a way, which made them unable to account for the low suspension density used in the calculations. Merry's (1975) correlation in turn resulted in too high penetration length values. However, there proved to be too many uncertainties, with both the starting values and the results, to confidently employ any of the tested correlations in the calculation tool.

All the goals set for the calculation tool development were met. To promote usability, a comprehensive calculation guide was written to accompany the tool, and all inputs possible were limited to predetermined choices to limit human error. Simultaneously it was made to account for more advanced design choices, without sacrificing usability. To achieve better penetration length evaluations, the evaluation method was developed further to account for a wider range of nozzle sizes and to allow better visualization of the results. The final calculation tool was tested and successfully used during the calculations of a new boiler proposal.

References

Alakangas, E., Hurskainen, M., Laatikainen-Luntama, J., Korhonen, J., 2016. Suomessa käytettävien polttoaineiden ominaisuuksia, VTT Technology. VTT Oy.

ASCE: Air and Gas Duct Structural Design Committee, 2020. Structural Design of Air and Gas Ducts for Power Stations and Industrial Boiler aplications, 2nd ed. American Society of Civil Engineers, Reston, Virginia.

Azad, A.K., Rasul, M.G., 2019. Advanced biofuels: applications, technologies and environmental sustainability, Woodhead publishing series in energy. Woodhead publishing, Duxford.

Basu, P., 2015. Circulating Fluidized Bed Boilers: Design, Operation and Maintenance, 1st ed. 2015. ed. Springer International Publishing : Imprint: Springer, Cham. https://doi.org/10.1007/978-3-319-06173-3

Basu, P., 2006. Combustion and gasification in fluidized beds. Boca Raton: CRC/Taylor & Francis.

Basu, S., Debnath, A.K., 2019. Power plant instrumentation and control handbook: a guide to thermal power plants, Second edition. ed. Academic Press, London [England] ; San Diego, CA.

Benjelloun, F., Liegeois, R., Vanderschuren, J., 1995. Penetration Length of Horizontal Gas Jets into Atmospheric Fluidized Beds. Proc Fluid.-VIII 239–246.

Bröckl, M., Kiuru, H., Heads, S., Kämäräinen, K., Patronen, J., Luoma-aho, K., Armila, N., Sipilä, E., Semkin, N., 2021. Jätteenpolton kiertotalous ja ilmastovaikutuksiin vaikuttaminen eri ojhjauskeinoin, Valtioneuvoston selvitys- ja tutkimustoiminnan julkaisusarja. Valtioneuvoston kanslia, Helsinki.

Cahyadi, A., Neumayer, A.H., Hrenya, C.M., Cocco, R.A., Chew, J.W., 2015. Comparative study of Transport Disengaging Height (TDH) correlations in gas–solid fluidization. Powder Technol. 275, 220–238. https://doi.org/10.1016/j.powtec.2015.02.010

Dawe, M., Briens, C., Berruti, F., 2008. Study of horizontal sonic gas jets in gas–solid fluidized beds. Can. J. Chem. Eng. 86, 506–513. https://doi.org/10.1002/cjce.20065

Heselton, K., 2014. Boiler operator's handbook, 2nd ed. The fairmont Press, Lilburn, Georgia.

Hong, R., Li, Hongzhong, Li, Haibin, Wang, Y., 1997. Studies on the inclined jet penetration length in a gas—solid fluidized bed. Powder Technol. 92, 205–212. https://doi.org/10.1016/S0032-5910(97)03238-5

Huhtinen, M., 2000. Höyrykattilatekniikka, 5th ed. Edita, Helsinki.

Khan, A.A., 2009. Biomass combustion in fluidized bed boilers: Potential problems and remedies. Fuel Process. Technol. 90, 21–50. https://doi.org/10.1016/j.fuproc.2008.07.012

Koornneef, J., Junginger, M., Faaij, A., 2007. Development of fluidized bed combustion—An overview of trends, performance and cost. Prog. Energy Combust. Sci. 33, 19–55. https://doi.org/10.1016/j.pecs.2006.07.001

Lewis, W.K., Gilliland, E.R., Lang, P.M., 1962. . Chem. Eng. Prog. Symp. Ser. 65.

Liimatainen P, 2022. Email conversation.

Lindsley, D., Grist, J., Parker, D., 2018. Thermal power plant control and instrumentation: the control of boilers and HRSGs, 2nd edition. ed, IET energy engineering. Institution of Engineering and Technology, Stevenage.

Merry, J.M.D., 1971. Penetration of a Horizontal Gas Jet into a Fluidized Bed. Trans Inst Chem 49, 189–195.

Nasrullah, M., Vainikka, P., Hannula, J., Hurme, M., Kärki, J., 2015. Mass, energy and material balances of SRF production process. Part 3: Solid recovered fuel produced from municipal solid waste. Waste Manag. Res. J. Sustain. Circ. Econ. 33, 146–156. https://doi.org/10.1177/0734242X14563375

Pena, P., 2011. Bubbling fluidized beds: When to use this technology. Presented at the Industrial Fluidization South Africa, Southern African Institute of Mining and Metallurgy, Johannesburg, pp. 57–66.

Perry, R.H., Green, D.W., Maloney, J.O. (Eds.), 1997. Perry's chemical engineers' handbook, 7th ed. ed. McGraw-Hill, New York.

Raiko, R., International Flame Research Foundation, Suomen kansallinen osasto, 1995. Poltto ja palaminen. Teknillisten tieteiden akatemia, Helsinki.

Röser, D., 2008. Sustainable use of forest biomass for energy: a synthesis with focus on the Baltic and Nordic region, Managing forest ecosystems. Springer, Dordrecht, the Netherlands.

Saario, A., 2008. Mathematical modeling and multiobjective optimization in development of low-emission industrial boilers: thesis for the degree of Doctor of Technology to be presented with due permision for public examination and criticism in Konetalo Building, Auditorium K1703, at Tampere University of Technology, on the 16th of May 2008, at 12 noon. Tampereen teknillinen yliopisto, Tampere.

Savolainen, K., Karvinen, R., 2001. Experimental and numerical studies of particle turbulence interaction and jet penetration in gas-particle flow. Trans. Eng. Sci. 30.

Scala, F., 2013. Fluidized bed technologies for near-zero emission combustion and gasification, Woodhead Publishing Series in Energy. Woodhead Pub., Philadelphia.

Sher, F., Liu, Hao, Sun, C., Afilaka, D.T., Pans, M.A., 2017. Experimental investigation of woody and non-woody biomass combustion in a bubbling fluidised bed combustor focusing on gaseous emissions and temperature profiles. Energy 14, 2069–2080. https://doi.org/10.1016/j.energy.2017.11.118

Simonen, M., 1999. Jet penetration in gas-particle suspension. (M. Sc. Thesis). Tampere University of Technology, Tampere.

Sumitomo SHI FW, 2022. Internal materials.

Teir, S., 2003. Steam boiler technology. Helsinki University of Technology, Espoo.

Vakkilainen, E., 2016. Steam Generation from Biomass: Construction and Design of Large Boilers. Oxford: Elsevier Science & Technology.

Vallero, D.A., 2014. Fundamentals of air pollution, 5th edition. ed. Elsevier, Amsterdam Boston.

Wang, S., Yang, Q., Shao, B., Zhao, J., Liu, L., Liu, Y., 2015. Numerical simulation of horizontal jet penetration using filtered fluid model in gas–solid fluidized bed. Powder Technol. 276, 1–9. https://doi.org/10.1016/j.powtec.2015.02.009

Yates, J.G., Gobbinah, S.S., Cheesman, D.J., Jordan, S.P., 1988. Particle Attrition in Fluidized Beds Containing Opposing Jets. AIChE Symp Ser 281, 13–19.

Zenz, F.A., 1968. Bubble Formation and Grid Design. Inst Chem Eng Symp Ser 30, 136–139.